J Automobile Engineering 2018, Vol. 232(13) 1762–1781

Determination of critical operating and geometrical parameters in diesel injectors through one dimensional modelling, design of experiments and an analysis of variance

Francisco J Salvador, Marcos Carreres, Marco Crialesi-Esposito and Alejandro H Plazas

CMT-Motores Térmicos. Universitat Politècnica de València, Spain

Corresponding author:

Dr. Francisco Javier Salvador

CMT-Motores Térmicos, Universitat Politècnica de València

Email: fsalvado@mot.upv.es

Abstract

In this paper, a design of experiments and a statistical analysis of variance (ANOVA) are performed to determine the parameters that have more influence on the mass flow rate profile in diesel injectors. The study has been carried out using a one dimensional model previously implemented by the authors. The investigation is split into two different parts. First, the analysis is focused on functional parameters such as the injection and discharge pressures, the energizing time and the fuel temperature. In the second part, the influence of 37 geometrical parameters such as the diameters of hydraulic lines, calibrated orifices and internal volumes, among others, are analysed. The objective of the study is to quantify the impact of small variations in the nominal value of these parameters on the injection rate profile for a given injector operating condition. In the case of the functional parameters, these small variations may be attributed to possible undesired fluctuations in the conditions that the injector is submitted to. As far as the geometrical and flow parameters are concerned, the small variations studied are representative of manufacturing tolerances that could influence the injected mass flow rate.

As a result, it has been noticed that the configuration of the inlet and outlet orifices of the control volume together with the discharge coefficient of the inlet orifice, among a few others, play a remarkable role in the injector performance. The reason resides in the fact that they are in charge of controlling the behaviour of the pressure in the control

volume, which importantly influences injector dynamics and therefore the injection process. Variations of only 5% in the diameter of these orifices strongly modify the shape of the rate of injection curve, influencing both the injection delay and the duration of the injection process, consequently changing the total mass delivered.

Keywords

injector, modelling, Diesel, dynamic, ANOVA

Nomenclature

A_o	Geometrical area
BP	Discharge pressure
C_c	Contraction coefficient
C_d	Discharge coefficient
CN	Cavitation number
D	Diameter
D_o	Geometrical nozzle diameter
ECU	Electronic Control Unit
ET	Energizing time

IT	Injection time
L	Length
LSD	Least Significant Difference
$\dot{m}_f$	Mass flow
OA	Outlet orifice
OZ	Inlet orifice
P_v	Vapour pressure
RBP	Return line discharge pressure
RP	Injection pressure
SOI	Start of injection
T	Fuel temperature
TMI	Total mass injected
u_B	Theoretical velocity, $u_B = \sqrt{\frac{2 \cdot (RP - BP)}{\rho_f}}$
V	Volume

Greek Symbols

ΔP	Pressure drop, $\Delta P=RP-BP$
ρ_f	Fuel density
υ_f	Fuel kinematic viscosity
λ	Flow coefficient or theoretical Reynolds number
	Subscripts
crit	Critical conditions

List of Tables

Table 1. Main specifications of the injector used for the study.

Table 2. Response variables considered for the analysis of mass flow rate.

Table 3. Functional parameters considered in the study.

Table 4. Geometrical and flow parameters considered for the analysis of variance.

List of Figures

Figure 1. Sketch and model of the needle.

Figure 2. Sketch and model of the injector holder.

Figure 3. Summary of the model validation against experimental results.

Figure 4. Definition of start of injection and injection time (injection duration).

Figure 5. Mass flow rate results of the L27 array for the study of functional parameters.

Figure 6. Mean value of SOI together with the LSD intervals for each factor considered.

Figure 7. Mean value of IT together with the LSD intervals for each factor considered.

Figure 8. Ratio between the control volume pressure and the rail pressure for the three levels of rail pressure considered.

Figure 9. Mean value of TMI together with the LSD intervals for each factor considered.

Figure 10. Total Mass Injected (TMI) as a function of the Rail Pressure (RP) and the Energizing Time (ET).

Figure 11. Mass flow rate results of the L81 array for the study of geometrical and flow parameters.

Figure 12. p-values for all the geometric parameters and LSD intervals for DOZ and DOA factors.

Figure 13. Pressure inside the control volume for different diameters of the control volume inlet orifice (OZ).

Figure 14. p-values for all the geometric parameters and LSD intervals for the significant factors DOZ, DOA and CDOZ.

Figure 15. p-values for all the geometric parameters and LSD intervals for the significant factors DOZ, CDOZ, DOA and DNO.

Figure 16. Mass flow rate profiles for the simulations of the L81 array without varying any of the parameters related to the control volume orifices.

Figure 17. p-values for all the geometric factors excluding the parameters of the control orifices.

Figure 18. LSD intervals for the CDOV2 factor.

Figure 19. LSD intervals for the VV2 factor.

Figure 20. LSD intervals for the CDOV1 factor.

Figure 21. LSD intervals for the DL4 and LL4 factors.

1. Introduction

Injection systems have a strong influence on the behaviour of the injection rate and thus in phenomena such as spray atomization, combustion and emissions (1)(2)(3)(4)(5)(6). It is therefore important to develop computational tools that enable to predict the behaviour of the system under different operating conditions, in order to optimise its performance and detect any potential problem (7)(8). Common-rail diesel injectors can be modelled by using a one-dimensional approach based on the Bond Graph technique (8)(9)(10). The capabilities of this kind of models have already been proved in several works published in the literature (8)(10) (11)(12)(13).

In the present investigation, the authors have utilized the potential of a Bosch injector 1D model previously developed and widely validated against experimental measurements (7)(9). Specifically, statistical methods (design of experiments and ANOVA analysis of variance) have been employed to quantify the sensitivity of the injection rate to variations in both the functional parameters and the design parameters (geometrical parameters). The variations in the values of these parameters that have been considered in this study correspond to a ±5% with respect to their nominal value. The intention of studying these variations is to quantify the effect on the injection rate of deviations around the nominal working parameters that could take place in a real engine for a given operating condition.

In the case of the functional parameters (injection pressure, energizing time, backpressure, return line or fuel temperature), there may be some uncertainties during a particular injection event. For instance, the high pressure pump may supply slightly different values of rail pressure for each stroke, influencing the injection rate to a certain extent. Also, the measurements carried out by the sensors used to control the injection pressure, cylinder pressure or current of the energizing signal sent by the injector to the ECU could be submitted to some errors. The studied range of the values of the parameters (5% around the nominal value) is expected to cover for this kind of possible deviations with respect to a nominal injection condition.

Similarly, in the case of the geometrical and flow parameters, the tolerances in the manufacturing process of the injector orifices or their obstruction due to depositions or coking could also influence their diameter and discharge coefficient within the ±5% range of variation considered. It is interesting then to quantify the influence of these deviations around the injector nominal geometry on the fuel mass delivery law for a given condition.

As far as the structure of the article is concerned, the structure of the injector and the proposed model are defined in Section 2 together with the response variables that help to parameterize the injection rate for its subsequent statistical analysis. Next, in Section 3, the designs of experiments used to analyse the functional and the geometrical parameters of the injector are defined. The statistical study of the variance carried out for both kinds of parameters is also presented in this section. The results and their detailed analysis are dealt with in Sections 4 and 5, devoted to the functional and the geometrical parameters, respectively. The conclusions of the study are finally condensed in Section 6.

2. Proposed model

The injector description, its operating principle, both its dimensional and hydraulic characterization and the steps followed for its modelling and validation are already published in (7). The injector dealt with in the study is a Bosch CRI 2.16 solenoid-operated injector (14), able to work at maximum pressures up to 160 MPa. Its main specifications are summarized in Table 1. It is important to highlight that, due to the internal similitude among diesel injectors, the results derived from this study are also applicable to other injectors (Delphi, Continental, Denso, etc.) to a certain extent. Sketches of part of the nozzle and the injector holder of the injector of study are represented in Figures 1 and 2, respectively. A summary of the validation against the experimental results presented in (7), both in terms of rate of injection and total mass injected, is shown in Figure 3.

Table 1. Main specifications of the injector used for the study.

Injector	Bosch CRI 2.16
Type	Solenoid-operated
Control valve type	Ball type valve
Max. operating pressure	160 MPa
Number of nozzle orifices	6
Nozzle orifices outlet diameter (nominal D_0)	131 µm

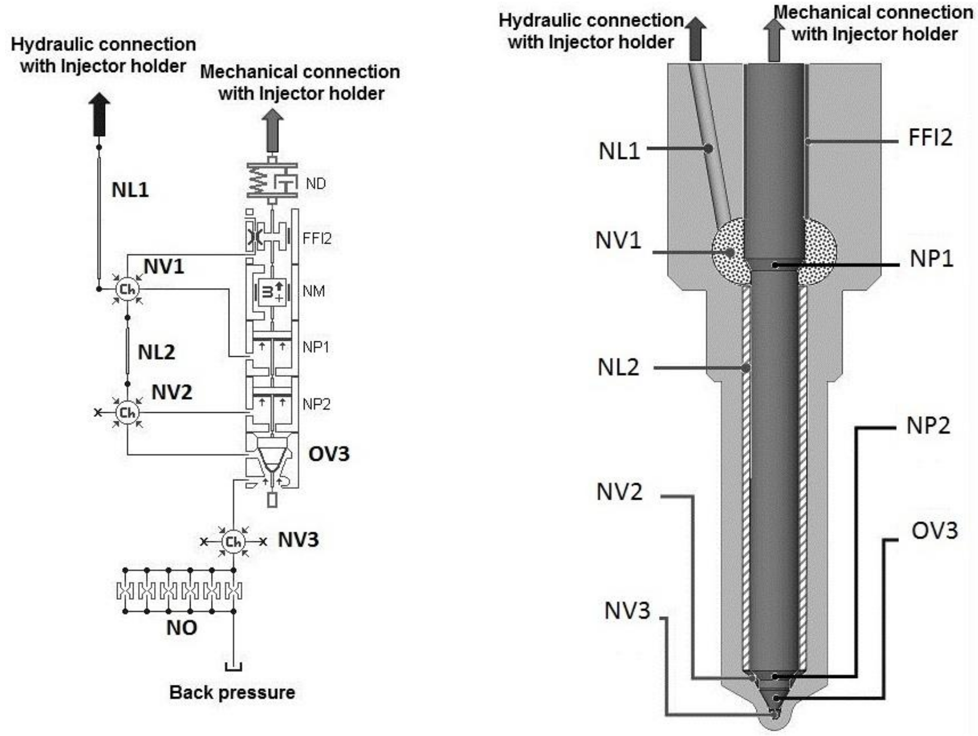

Figure 1. Sketch and model of the needle.

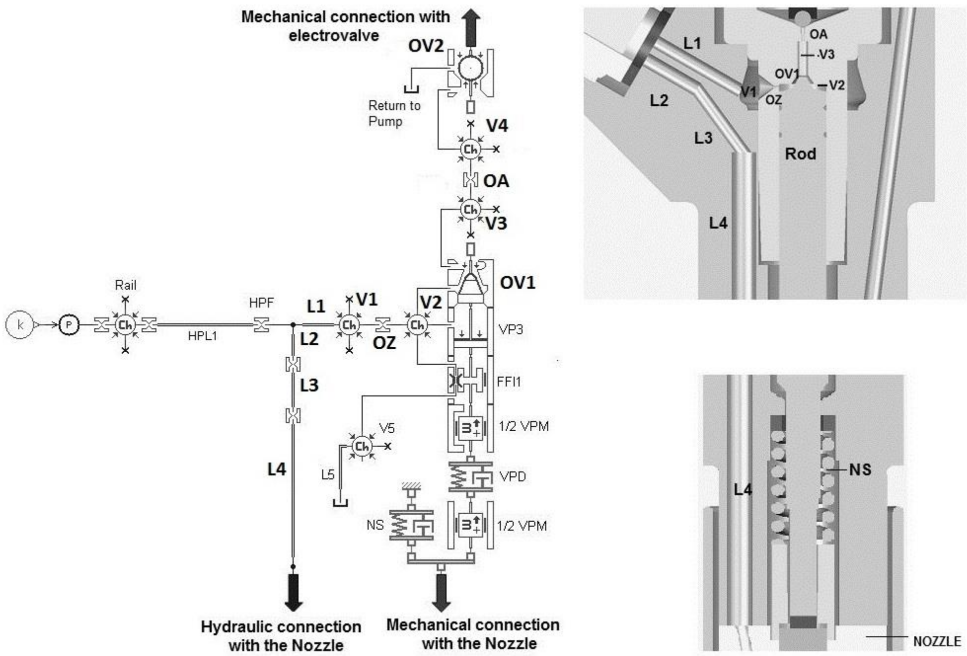

Figure 2. Sketch and model of the injector holder.

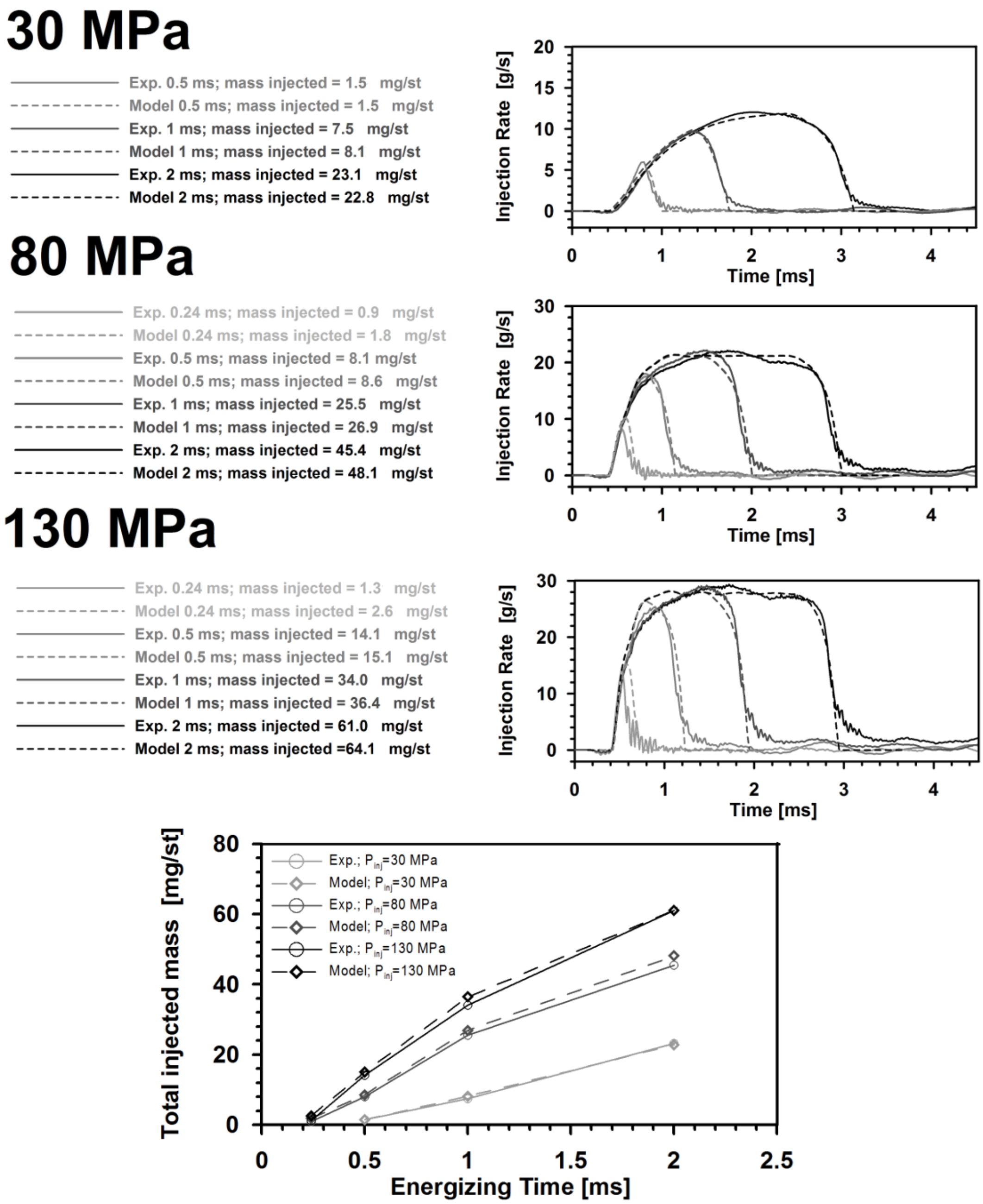

Figure 3. Summary of the model validation against experimental results.

The parameters employed as response variables on which the analysis of variance is carried out are those that define the rate of injection curve: start of injection (*SOI*), injection time (*IT*) and the total mass injected (*TMI*). These three variables are represented in Figure 4 for the experimental rate of injection curve (injection pressure of 80 MPa and energizing time of 1 ms). In this figure, the mass flow rate profile is depicted along with the intensity of the electrical current for some given injector operating conditions. As it can be seen in the figure, the start of injection (*SOI*) is defined as the delay between the start of the intensity signal and the start of the mass flow rate signal. The injection time (*IT*) is the elapsed time from the start of the injection to the end of the injection (i.e. the time during which the injector remains open). Finally, the total mass injected (*TMI*) corresponds to the integral over the time of the mass flow rate profile (shaded area below the mass flow rate profile).

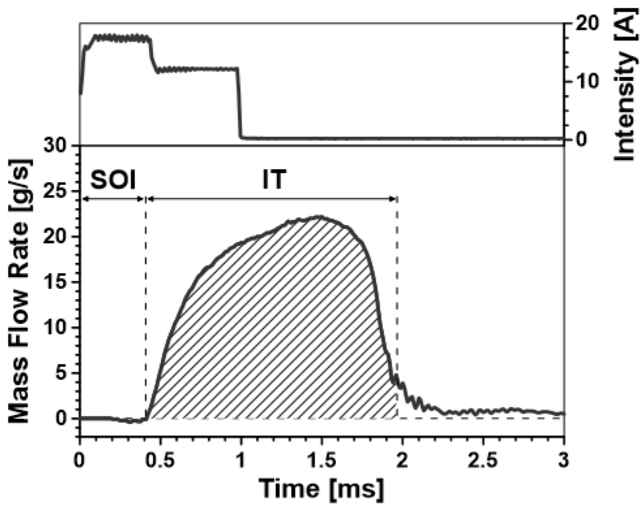

Figure 4. Definition of start of injection and injection time (injection duration).

The response variables considered in the study and their corresponding preferred units are summarized in Table 2. Please note that the term *mg/st* refers to the milligrams injected per injection cycle (stroke).

Table 2. Response variables considered for the analysis of mass flow rate.

Acronym	Meaning	Units
SOI	*Start of Injection*	*µs*
IT	*Injection Time*	*ms*
TMI	*Total Mass Injected*	*mg/st*

3. Design of experiments (DOE) and statistical analysis of variance (ANOVA)

5 operating parameters and 37 geometrical parameters with 3 different levels have been considered for the study. In order to study all the combinations between these parameters considering 3 levels for each parameter, it would have been necessary to perform 243 (3^5) simulations in the case of the functional parameters study and 4.5 10^{17} (3^{37}) simulations for the study of geometrical factors. In order to avoid this large quantity of tests, a design of calculations based on Taguchi theory was used (15). This technique, which allows carrying out experiments in a methodical way to obtain results at a minimum cost, was applied to define an appropriate set of simulations. Taguchi´s orthogonal array L_{27} was chosen to reduce the problem to 27 calculations in the first

case (functional parameters), and orthogonal array L_{81} was chosen for the study of geometric parameters to reduce the problem to 81 simulations in the second one (geometrical parameters). Arrays L_{27} and L_{81} allow to study up to 13 and 40 factors with 3 different levels, respectively. A statistical analysis of variance (ANOVA) of the data obtained from the simulations was performed in order to identify which parameters have more influence on the response variables summarized in Table 2.

4. Study on functional parameters

The parameters considered in this first part of the study are the rail pressure (*RP*), the energizing time (*ET*), the backpressure (*BP*), the fuel temperature (*T*) and the pressure existing in the injector return line (*RBP*). The location of the relevant pressures (*RP*, *BP* and *RBP*) was depicted in Figures 1 and 2. As far as the fuel temperature (*T*) is concerned, it must be noted that the model considers isothermal flow. Therefore, local variations in fuel temperature are not considered along a simulation.

For each of the factors, 3 different levels were chosen, comprising the nominal value and a variation of ±5 % over it. The nominal point corresponds to *RP* = 80 MPa, *ET*= 1ms, *T*= 40 ºC, *BP*= 40 bar and *RBP* = 0.07 MPa. Table 3 summarizes the different factors and levels considered for this study. All the possible combinations of all levels for all the factors lead to Taguchi's L_{27} array. Hence, 27 simulations are performed for the statistical study of the functional factors. Please note that each value of fuel temperature implies a given set of fluid properties (i.e. fuel density, viscosity and bulk modulus). Figure 5 depicts the mass flow rate profiles obtained for the 27 simulations of the L_{27} array.

Table 3. Functional parameters considered in the study.

Nº	**Factor**	**Acronym**	**Level 1**	**Level 2**	**Level 3**
1	Energizing Time (ms)	*ET*	0.95	1	1.05
2	Rail Pressure (MPa)	*RP*	76	80	84
3	Back Pressure (MPa)	*BP*	3.8	4.0	4.2
4	Temperature (ºC)	*T*	38	40	42
5	Return Back Pressure (MPa)	*RBP*	0.0665	0.07	0.0735

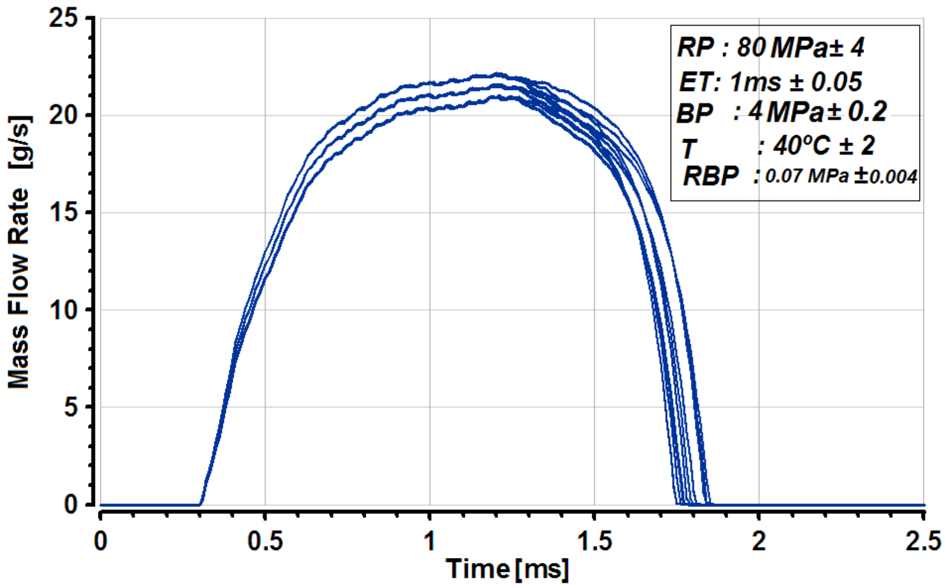

Figure 5. Mass flow rate results of the L_{27} array for the study of functional parameters.

A statistical analysis of variance (ANOVA) of the data obtained from the 27 simulations was performed in order to identify which parameters have more influence on the response variables.

4.1. Influence of functional parameters on the start of injection (SOI).

First, the contribution of each individual factor to the start of injection was studied and it may be summarized as follows: the factors *RP* and *T* have a statistically significant effect on the *SOI* at the 95% confidence level, whereas the analysis predicts a negligible influence of the factors *ET*, *BP* and *RBP* on the start of injection at the 95% confidence level.

In Figure 6, the mean value of *SOI* is represented for each level of the functional factors. The plots also display the Least Significant Difference (LSD) intervals for each of the mean values separately, with a confidence level of 95%. As shown in Figure 6, significant differences in the mean value of *SOI* are noticed when the values of the factors *RP* and *T* change and there is no superposition of the respective confidence intervals between different levels. This means that a fluctuation of the rail pressure or a variation in fuel temperature of about 5% is able to modify the start of injection significantly. Concerning the temperature, as it is visible in Figure 6, the value of *SOI* is lower when the temperature *T* is increased. This result was already observed by the authors by experimental means, as reported in (16). As analysed in (17) through the use of a 1D model of a similar injector to the one of the present investigation, this fact could be mainly attributed to the decrease in viscosity as the temperature increases. This implies a lower viscous friction, leading to a quicker opening of the injector needle. The effect of factors *ET*, *BP* and *RBP* is less significant, as represented by the overlap of the confidence interval for the different levels. The fact that the energizing time is not significant can be explained given that the variations on this factor are exclusively related to the duration of the electrical signal, therefore not affecting the properties of the signal in terms of maximum intensity level. In the case of the backpressure *BP*, a look at its LSD intervals reveals that the start of injection is smaller the higher the backpressure. This result is mainly due to the fact that the acting force on the tip of the needle is higher when the backpressure increases, leading to a higher needle opening force. Nevertheless, a variation of 5% does not significantly affect the start of injection. As far as the pressure in the return line is concerned, its influence is almost negligible. In this case, the explanation has to do with the cavitation regime under which the orifice located upstream of the return line works. This orifice (*OA* in Figure 2) normally works under cavitation regime due to the low downstream pressures (around 0.07 MPa for the injector used in this investigation) and high upstream pressures achieved. According to the cavitation theory, in such conditions the mass flow does not further depend on the pressure downstream (18). Thus, any variation in this parameter does not affect the mass flow rate, as has been observed.

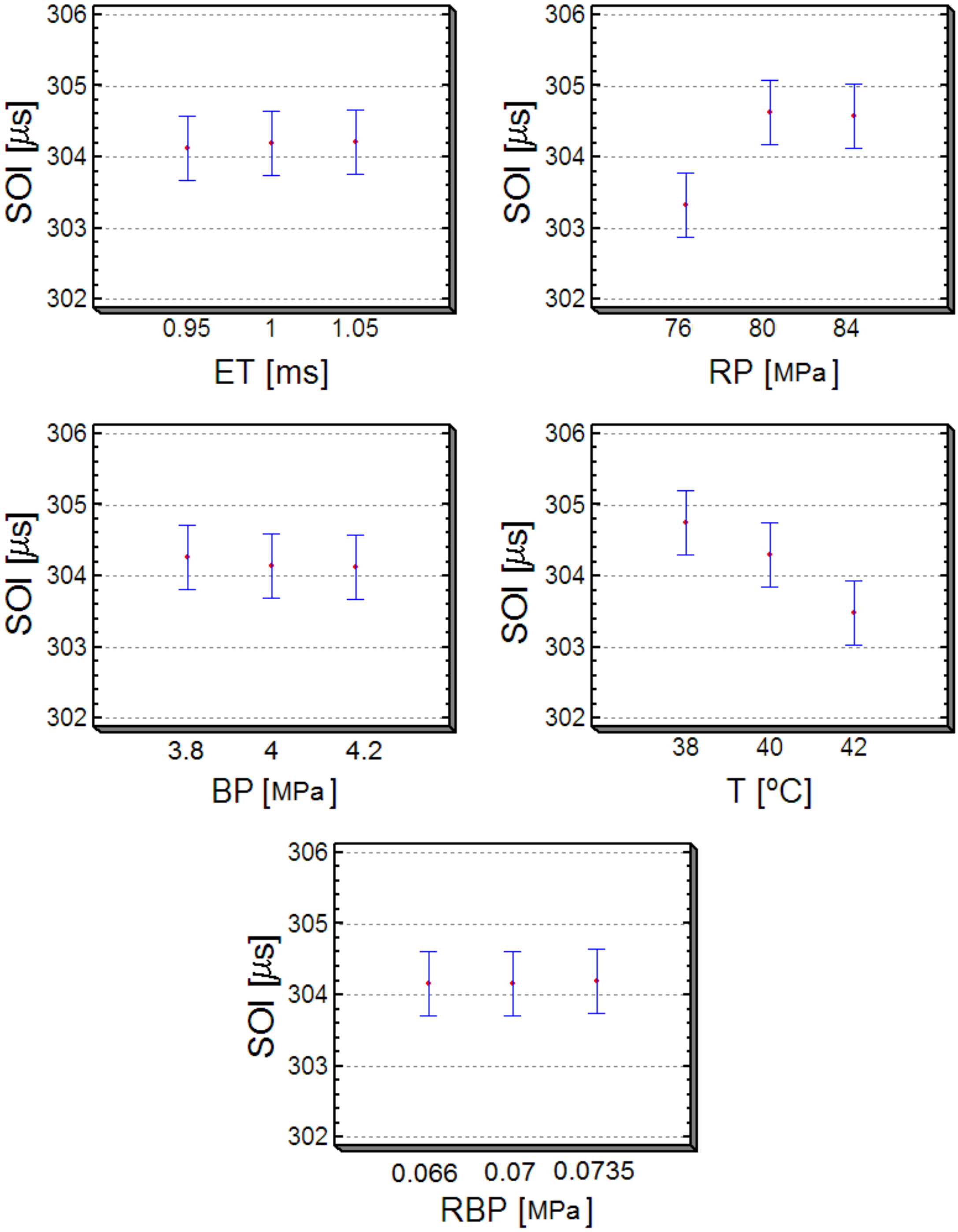

Figure 6. Mean value of *SOI* together with the LSD intervals for each factor considered.

4.2 Influence of functional parameters on the injection duration (IT).

Following the same procedure as in the case of the start of injection, an analysis of variance has been also performed for the injection time. In this case, the LSD intervals are displayed in Figure 7 for all the factors. As can be clearly noted, the factors *RP* and *ET* have a statistically significant effect on the *IT* at the 95% confidence level. Regarding the other factors (*T, BP* and *RBP*), the analysis predicts that their influence on the injection duration is negligible at the 95% confidence level. As far as the energizing time influence is concerned, its influence on the injection time seems obvious, since the energizing time is closely related to the injection time, whereas in the case of the rail pressure its influence is due to the fact that when the injection pressure increases, the force acting on the needle tip is higher at the moment of the injector opening. Thus, the needle velocity increases during this first stage of the injection. Consequently, the rod (Figure 2) moves further upwards during this first part of the injection, thus reducing the size of the control volume at the ball valve closing stage (end of energizing time). As a result of the control volume reduction, the pressure in it gets higher, as represented in Figure 8, which shows the ratio among the control volume pressure (*CVP*) and the rail pressure (*RP*) for the 3 pressure levels considered. This pressure increase in the control volume entails a bigger force on the upper part of the rod (see Figure 2) and therefore a quicker needle closing.

With regard to the non-significant factors over the injection time, a slight increment of the injection time when the backpressure *BP* is increased can be noted according to Figure 7. As it was stated earlier, the higher the backpressure, the larger the force acting on the needle tip (NV3 volume in Figure 1). This would entail a bigger needle speed in the opening phase. Nevertheless, during the closing phase, this same force opposes the needle movement resulting in a longer time needed to close the injector. Consequently, the injection time becomes larger. On the other hand, the influence of the temperature *T* on this parameter is mainly due to viscosity variations. The viscosity is reduced the larger the fuel temperature, thus lessening the fuel viscous friction between the needle and the wall and also in the gap between the rod and the wall of the injector holder. As a result, the maximum needle lift increases leading to longer injection durations.

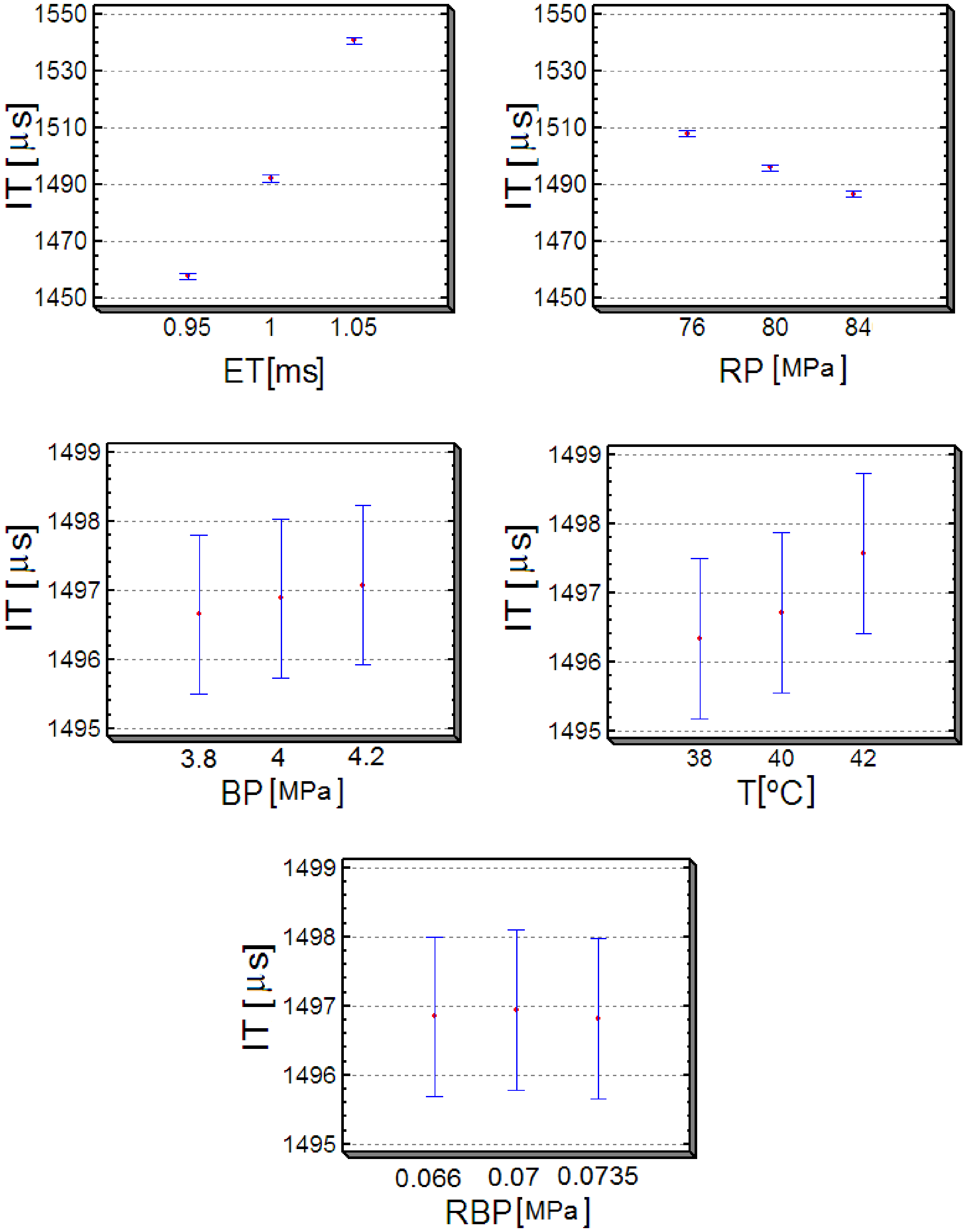

Figure 7. Mean value of *IT* together with the *LSD* intervals for each factor considered.

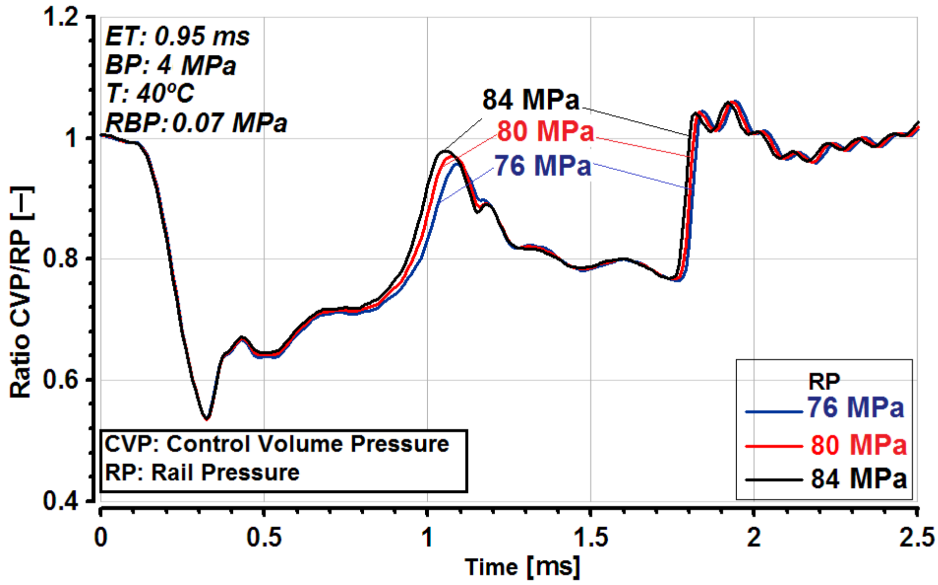

Figure 8. Ratio between the control volume pressure and the rail pressure for the three levels of rail pressure considered.

4.3 Influence of functional parameters on the total mass injected (TMI).

As per the total mass injected, the analysis according to the LSD intervals displayed in Figure 9 showed that the variables that influence it in a more important manner are the energizing time (*ET*) and the rail pressure (*RP*), as it happened for the injection duration. This result is somehow expected since these variables are the ones directly controlled by the ECU of the engine in order to get a certain mass of fuel injected. Figure 10 shows the variation in the total mass injected quantity as a function of the rail pressure and the energizing time when the values of the other functional factors (*BP*, *T* and *RBP*) are kept constant. As it can be seen, the energizing time should be reduced if it is desired to keep constant the injected mass when increasing the rail pressure.

With regard to the non-significant effects on the total mass injected, Figure 9 shows that the effects of the temperature and backpressure are small but clear. As far as the backpressure is concerned, its increase leads to a reduction in total mass injected due to the reduction of the pressure drop under which the nozzle works. In the case of the temperature, larger values result in an increase in total mass injected due to the larger injection times achieved as found in Section 4.2.

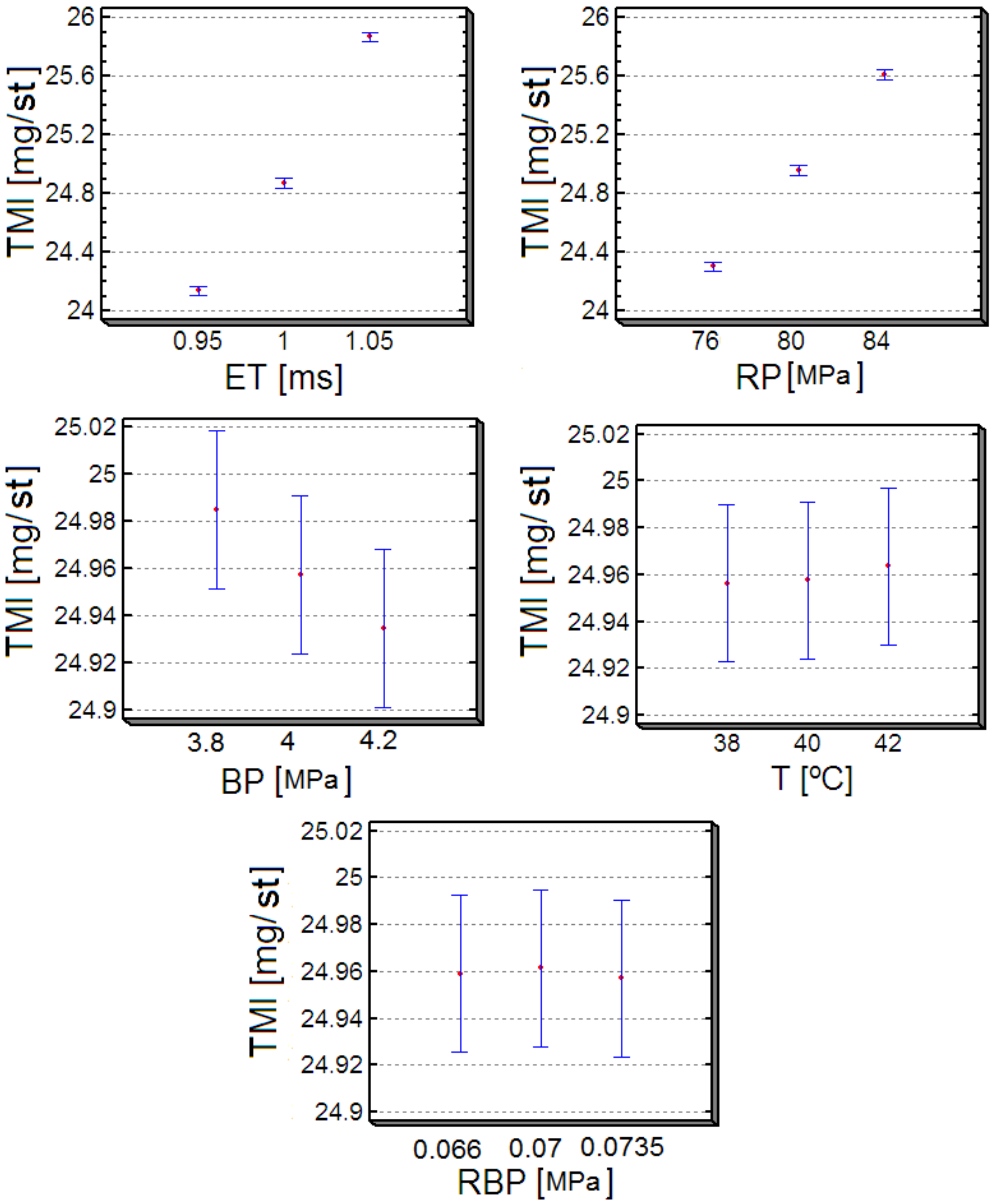

Figure 9. Mean value of *TMI* together with the LSD intervals for each factor considered.

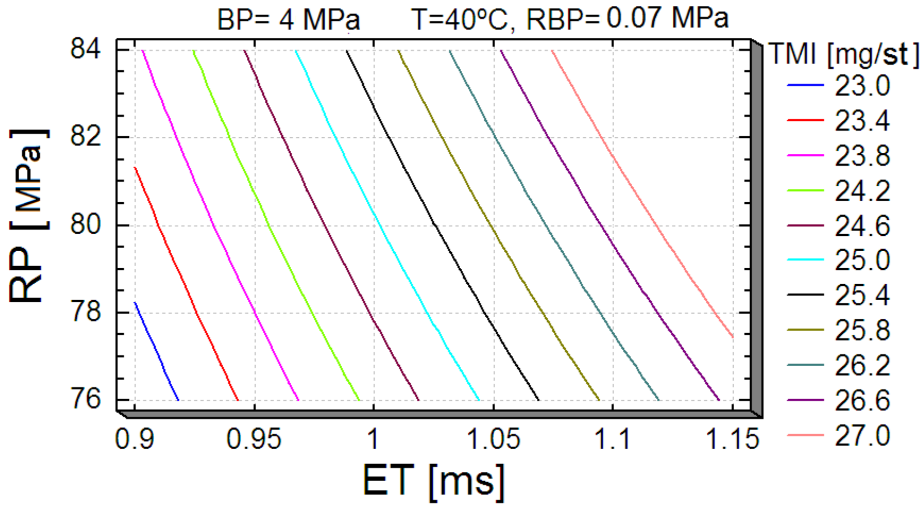

Figure 10. Total Mass Injected (*TMI*) as a function of the Rail Pressure (*RP*) and the Energizing Time (*ET*).

5. Study on geometrical parameters

Once the influence of the functional parameters has been analysed, the same type of study has been carried out in this section in order to determine which geometrical parameters have more influence on the injection rate.

The parameters selected in this case are classified into two categories. On the one hand, pure geometrical parameters such as lengths and diameters of lines, internal volumes in the nozzle and the injector holder, roughness of lines and diameter of control volume orifices, among others. The elements containing these parameters are highlighted in bold letters in the schemes showed at the left of Figures 1 and 2. On the other hand, for some of the orifices deemed to have a great influence on the behaviour of the injector, important hydraulic parameters (aside from the diameter) have also been included in this part of the study. This is the case of the maximum discharge coefficient, the critical cavitation number and the critical flow number. The elements containing them are the nozzle orifices (*NO* in Figure 1), the control volume orifices (*OA* and *OZ* in Figure 2) and different variable orifices (*OV1*, *OV2* and *OV3* in Figures 1 and 2) for which the area depends on the lift of movable pieces (needle, rod or command piston). As it is well known, the discharge coefficient for an orifice under non-cavitating conditions exhibits an asymptotic behaviour when plotted against the Reynolds number (6)(7)(8)(13), so that it reaches a maximum value (C_{dmax}) once the Reynolds number is high enough. The critical flow number is defined as the value of flow number that leads to a discharge coefficient value of 95% of C_{dmax}.

This flow number (λ) can be regarded as a theoretical Reynolds number for which Bernoulli's theoretical velocity is considered instead of the actual velocity, according to Equation (1):

$$\lambda = \frac{D_o}{\nu_f} \cdot \sqrt{\frac{2 \cdot (RP - BP)}{\rho_f}} \qquad (1)$$

where *RP* and *BP* are the rail pressure and the backpressure (or discharge pressure), respectively. As far as the cavitation number is concerned, the definition introduced by Soteriou et al. (19) has been considered in this study:

$$CN = \frac{RP - BP}{BP - P_v} \tag{2}$$

The vapour pressure is usually neglected due to its small value when compared to both the rail pressure and the discharge pressure. The critical cavitation number (CN_{crit}) corresponds to the pressure drop for which cavitation starts. An acceptable estimation of these conditions can be experimentally determined through the stabilization of the mass flow rate or mass flow choking (18)(20)(21)(22)(23)(24)(25)(26). As previously established, when an orifice does not cavitate, the discharge coefficient increases with the Reynolds number (or flow number) (27)(28)(29). However, under cavitating conditions (i.e. when $CN > CN_{crit}$) the discharge coefficient stops increasing with the Reynolds number and varies (decreases) with the cavitation number as described by Equation (3) (30)(31)(32)(33)(34):

$$C_d = C_c \cdot \sqrt{1 + \frac{1}{CN}} \tag{3}$$

where C_c is a coefficient that quantifies the contraction that takes place in the orifice due to cavitation. C_c may be obtained by particularizing the equations for the critical cavitation conditions (CN_{crit}), for which the discharge coefficient is known.

All these geometric and hydraulic parameters are compiled in Table 4 with the nomenclature established for each element of the model in Figures 1 and 2. Data referring to hydraulic parameters are represented in grey background at the bottom of the table. As done in Section 4 for the functional parameters, the nominal value is represented in this table (level 2) together with the levels corresponding to ± 5% of variation (level 1 and 3).

Table 4. Geometrical and flow parameters considered for the analysis of variance.

Nº	Component	Factor	Nom.	Level 1	Level 2	Level 3
1	Line L1	Diameter (mm)	*DL1*	1.3680	1.4400	1.5120
2		Length (mm)	*LL1*	7.1915	7.5700	7.9485
3	Line L2	Diameter (mm)	*DL2*	1.1590	1.2200	1.2810
4		Length (mm)	*LL2*	6.8590	7.2200	7.5810
5	Line L3	Diameter (mm)	*DL3*	1.0545	1.1100	1.1655
6		Length (mm)	*LL3*	3.2205	3.3900	3.5595
7	Line L4	Diameter (mm)	*DL4*	2.0520	2.1600	2.2680
8		Length (mm)	*LL4*	109.2500	115.0000	120.7500
9	Line NL1	Diameter (mm)	*DNL1*	2.0520	2.1600	2.2680
10		Length (mm)	*LNL1*	14.2500	15.0000	15.7500
11	Line NL2	Diameter (mm)	*DNL2*	2.2800	2.4000	2.5200
12		Length (mm)	*LNL2*	25.6500	27.0000	28.3500
13	Roughness	Roughness (mm)	*LR*	0.9500	1.0000	1.0500
14	Volume V1	Volume (mm^3)	*VV1*	118.7500	125.0000	131.2500
15	Volume V2	Volume (mm^3)	*VV2*	10.9060	11.4800	12.0540

16	Volume V3	Volume (mm^3)	*VV3*	2.2230	2.3400	2.4570
17	Volume V4	Volume (mm^3)	*VV4*	0.0536	0.0565	0.0592
18	Volume NV1	Volume (mm^3)	*VNV1*	30.8750	32.5000	34.1250
19	Volume NV2	Volume (mm^3)	*VNV2*	4.7756	5.0270	5.2783
20	Volume NV3	Volume (mm^3)	*VNV3*	0.0554	0.0584	0.0613
21	Inlet control orifice	Diameter (μm)	*DOZ*	205.2000	216.0000	226.8000
22	OZ	Cd_{max}	*CDOZ*	0.6935	0.7300	0.7665
23		CN_{critic}	*CNOZ*	1.8620	1.9600	2.0580
24		λ_{critic}	*LOZ*	5937.5000	6250.0000	6562.5000
25	Outlet control	Diameter (μm)	*DOA*	233.7000	246.0000	258.3000
26	orifice OA	Cd_{max}	*CDOA*	0.8170	0.8600	0.9030
27		CN_{critic}	*CNOA*	5.1775	5.4500	5.7225
28		λ_{critic}	*LOA*	9025.0000	9500.0000	9975.0000
29	Nozzles orifices	Diameter (μm)	*DNO*	124.4500	131.0000	137.5500
30	NO	Cd_{max}	*CDNO*	0.7790	0.8200	0.8610
32		λ_{critic}	*LNO*	4845.0000	5100.0000	5355.0000
33	Variable orifice	Cd_{max}	*CDOV3*	0.5700	0.6000	0.6300
34	OV3	λ_{critic}	*LOV3*	950.0000	1000.0000	1050.0000
35	Variable orifice	Cd_{max}	*CDOV2*	0.5700	0.6000	0.6300
36	OV2	λ_{critic}	*LOV2*	950.0000	1000.0000	1050.0000
37	Variable orifice	Cd_{max}	*CDOV1*	0.5700	0.6000	0.6300
38	OV1	λ_{critic}	*LOV1*	950.0000	1000.0000	1050.0000

This analysis is performed on the nominal point used for the study about functional parameters: *RP* = 80 MPa, *ET* = 1ms, *T* = 40ºC, *BP* = 4 MPa and *RBP* = 0.07 MPa.

The L_{81} Taguchi´s Orthogonal array (15) was chosen for the study of geometric parameters in order to reduce the problem to 81 simulations instead of 50653 (37^3).

The mass flow rate profiles provided by the simulations corresponding to the L_{81} array are displayed in Figure 11. As it can be seen, a variation of just a 5% in the nominal values entails an important variation in the mass flow rate behaviour. The results of the ANOVA on each of the response variables considered (start of injection, injection time and total mass injected) are presented and analysed in the following subsections.

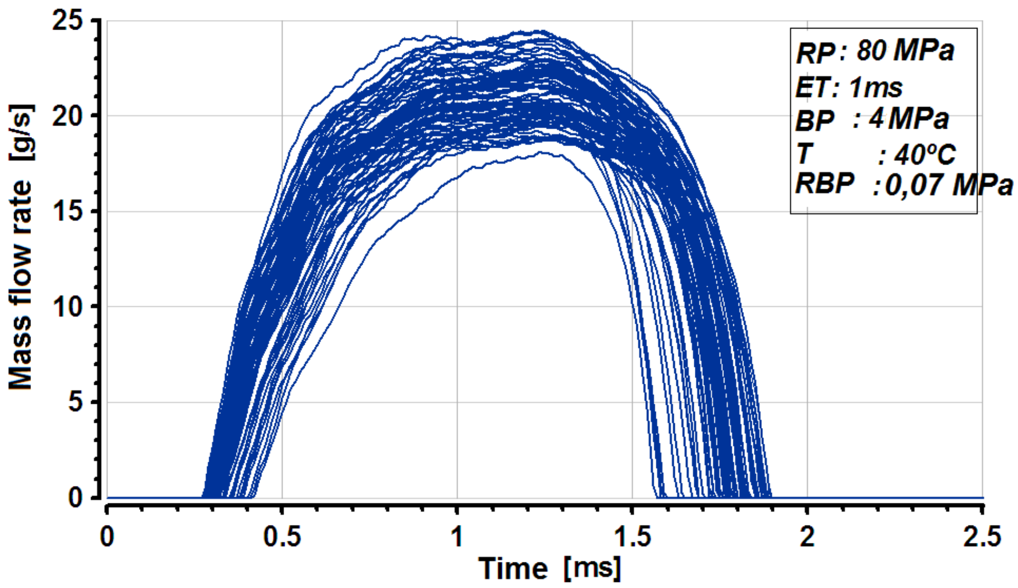

Figure 11. Mass flow rate results of the L_{81} array for the study of geometrical and flow parameters.

5.1. Influence of geometrical parameters on the start of injection (SOI).

The results of the study on the contribution of each geometrical factor to the start of injection response variable are summarized in Figure 12 through the *p-values*. Factors with *p-values* lower than 0.05 have a statistically significant effect on the *SOI*. Therefore, only the factors *DOZ* and *DOA* (diameters of the inlet and outlet orifices of the control volume, respectively) have a statistically significant effect on the *SOI* at the 95% confidence level. The diameters of these orifices are followed in importance by their corresponding discharge coefficients which (despite not being significant from the statistical point of view) have much more influence on the start of injection than the rest of parameters, for which the analysis predicts a negligible influence at the 95% confidence level. The mean values of *SOI* for each level of the *DOZ* and *DOA* are represented at the bottom part of Figure 12 together with the corresponding LSD intervals with a confidence level of 95%.

As shown by the LSD intervals, it can be noted that the start of injection greatly increases when the diameter of the control volume inlet orifice (*DOZ*) becomes higher, whereas the contrary is seen when referring to the control volume outlet orifice (*DOA*). In this case, if the *DOA* gets higher, the start of the injection is considerably reduced. In order to explain this behaviour, the pressure registered inside the control volume (*V2* in Figure 2) is displayed in Figure 13 for the three different values of *DOZ* and the nominal operating conditions. As mentioned earlier, this pressure is deemed to have an important influence on injector dynamics since it is directly related to the force exerted on the upper part of the rod (Figure 2). This pressure force, together with the one exerted on the bottom part of the needle (Figure 1), determines the dynamic behaviour of the needle-rod ensemble.

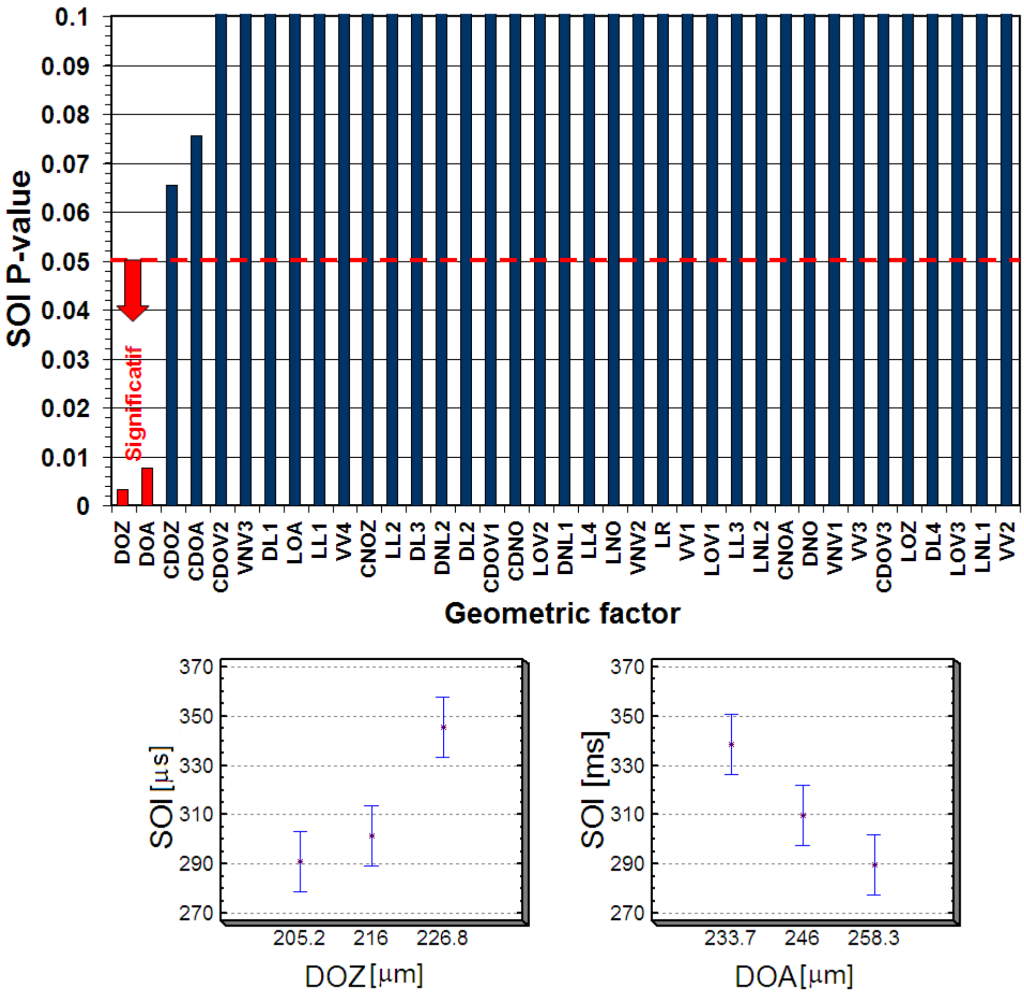

Figure 12. *p-values* for all the geometric parameters and LSD intervals for *DOZ* and *DOA* factors.

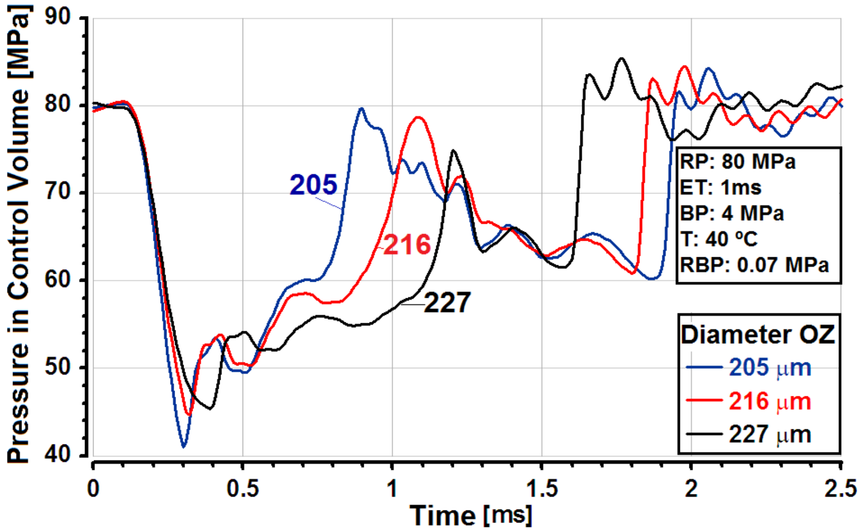

Figure 13. Pressure inside the control volume for different diameters of the control volume inlet orifice (OZ).

As can be seen from the Figure, the smaller the diameter of the OZ orifice, the bigger the pressure drop along this orifice during the beginning of the injection, just when the OA orifice has been released by the opening of the ball valve *OV2* (Figure 2) as a result of the injector energizing. As a consequence, the smaller the OZ diameter, the lower the pressure inside the control volume. This results in a lower force exerted on the upper part of the rod, which opposes to the needle opening thus reducing the time needed for the injector to open.

The same effect is observed for the control volume outlet orifice (*OA*) with opposite consequences. In this particular case, given that this orifice is connecting the control volume to the return line through the ball valve, the bigger the diameter, the lower the pressure reached inside the control volume. Therefore, the quicker the needle moves upwards thus advancing the start of the injection.

5.2. Influence of geometrical parameters on the injection duration (IT).

As far as the influence on the injection duration is concerned, the results of the ANOVA in terms of the *p-value* are given in Figure 14. In this case, three significant factors have been found: the diameters of the control volume inlet and outlet orifices and the discharge coefficient of the first one. The control volume inlet orifice diameter (*DOZ*) is, by far, the parameter which mostly affects the injection duration, followed by its discharge coefficient and finally the control volume outlet orifice. The rest of parameters resulted not to be significant (*p-value* higher than 0.05). The importance of *DOZ* on the injection duration is revealed when looking at the LSD intervals in Figure 14. The fact that these intervals do not show any type of overlapping among them when changing from a value of *DOZ* to another one means that the injection time is greatly affected by this modification regardless of the variation in any other parameter. In the case of the discharge coefficient of the *OZ* orifice (*CDOZ*), the LSD intervals are less separated, with a small superposition among them as shown in the bottom part of Figure 14. Finally, the diameter of the *OA* orifice (*DOA*), the third in importance, exhibits LSD intervals with higher level of superposition among them.

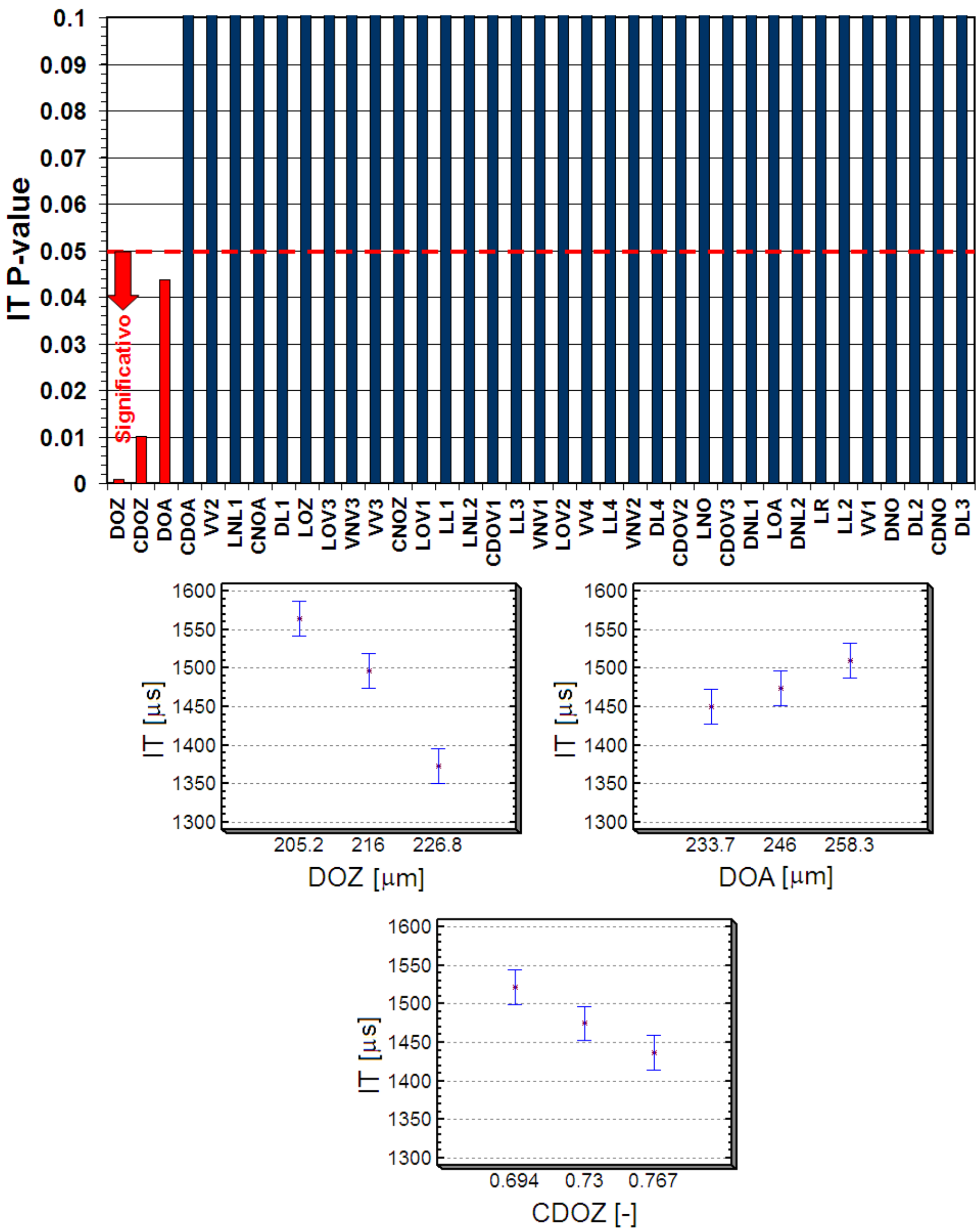

Figure 14. *p-values* for all the geometric parameters and LSD intervals for the significant factors *DOZ*, *DOA* and *CDOZ*.

As it happened in previous cases, another important observation is how the injection duration changes when the values of each factor are modified. As noticeable from observing the LSD intervals, the injection duration is lower when the control volume inlet orifice diameter (or its discharge coefficient) is increased, whereas it grows when the control volume outlet diameter is increased. Regarding the inlet orifice, the cause of this behaviour has to do with the aforementioned phenomenon: as the inlet diameter gets larger, the pressure losses through it become smaller. Therefore, a higher pressure is found inside the control volume during the opening stage, as can be seen in Figure 13 (time interval between 0.2 and 0.4 ms). This pressure acts on the upper part of the rod. As a result, the difference between the pressure acting on the needle tip (volume *NV2* in Figure 1) and the one acting on the upper part of the rod (in the control volume, *V2* in Figure 2) decreases. Consequently, the needle is slowed down during the injector opening phase. The delay between the different signals is directly related to the start of injection (*SOI*) parameter previously analysed in Section 5.1. Nonetheless, the injection time (*IT*) depends not only on what happens internally during the opening stage, but also on the internal behaviour during the injector closing phase. Indeed, using larger *DOZ* values would result in a faster recovery of the pressure inside the control volume once the injector energizing is finished and the ball valve (*OV2* in Figure 2) has just closed, as can also be seen in Figure 13 (time interval between 1.5 and 2 ms). As a result, the needle speed is higher during the injector closing stage, thus cutting the injection process at an earlier stage and consequently reducing the injection duration.

In the case of the control volume outlet orifice (*OA*), the phenomenon that occurs inside the injector is somehow the opposite of that just described for the *OZ* orifice. In fact, when the *OA* diameter is increased, the pressure inside the control volume (*V2*) is lower (i.e. the pressure drop through the *OA* orifice is smaller). Hence, the injection starts sooner, increasing the injection duration. It is important to highlight that, in this case, this parameter only influences the needle opening stage. During the injector closing period, once the energizing time of the injector has finished, the ball valve is closed and there is no flow this orifice. As a result, no differences are observed in the injector closing part of the mass flow rate curves.

5.3 Influence of geometrical parameters on the total mass injected (TMI).

The results of the analysis of variance over the total mass injected (*TMI*) variable are compiled in Figure 15 through the *p-values* obtained for each factor considered. As it may be observed, the significant factors (*p-value* lower than 0.05) are, sorted by importance, the diameter of the control volume inlet orifice (*DOZ*), the diameter of the outlet orifice of the control volume (*DOA*), the discharge coefficient of the *OZ* orifice and the diameter of the nozzle orifices (*DNO*). In the bottom part of the figure, the LSD intervals of these significant factors are also shown. They highlight that the percentage of variation of the injected mass when modifying just a 5% in the diameters of the control orifices is in the order of 15%. This variation is more critical in the case of the inlet orifice (*DOZ*), whose LSD intervals do not show any overlapping among them. As it happened for the injection duration (*IT*), the effect of the inlet orifice (*OZ*) is greater than the effect of the outlet one (*OA*), given that the former is always active influencing needle dynamics, whereas the latter is only active during the period for which the ball valve is open (i.e. when the injector is electrically excited by the ECU signal).

As per the observed trends, these are similar to the ones reported in the previous study about the injection duration. When the diameter of the control volume inlet orifice (or its discharge coefficient) is increased, the total mass injected decreases. However, it is increased if the diameters of either the outlet orifice or the nozzle orifices are enlarged. The explanation in this last case is obvious, whereas the reason for the influence of the outlet orifice diameter is the previously explained variation in the control volume pressure when the control orifices are altered. To a certain extent, the total mass injected is closely related to the injection duration.

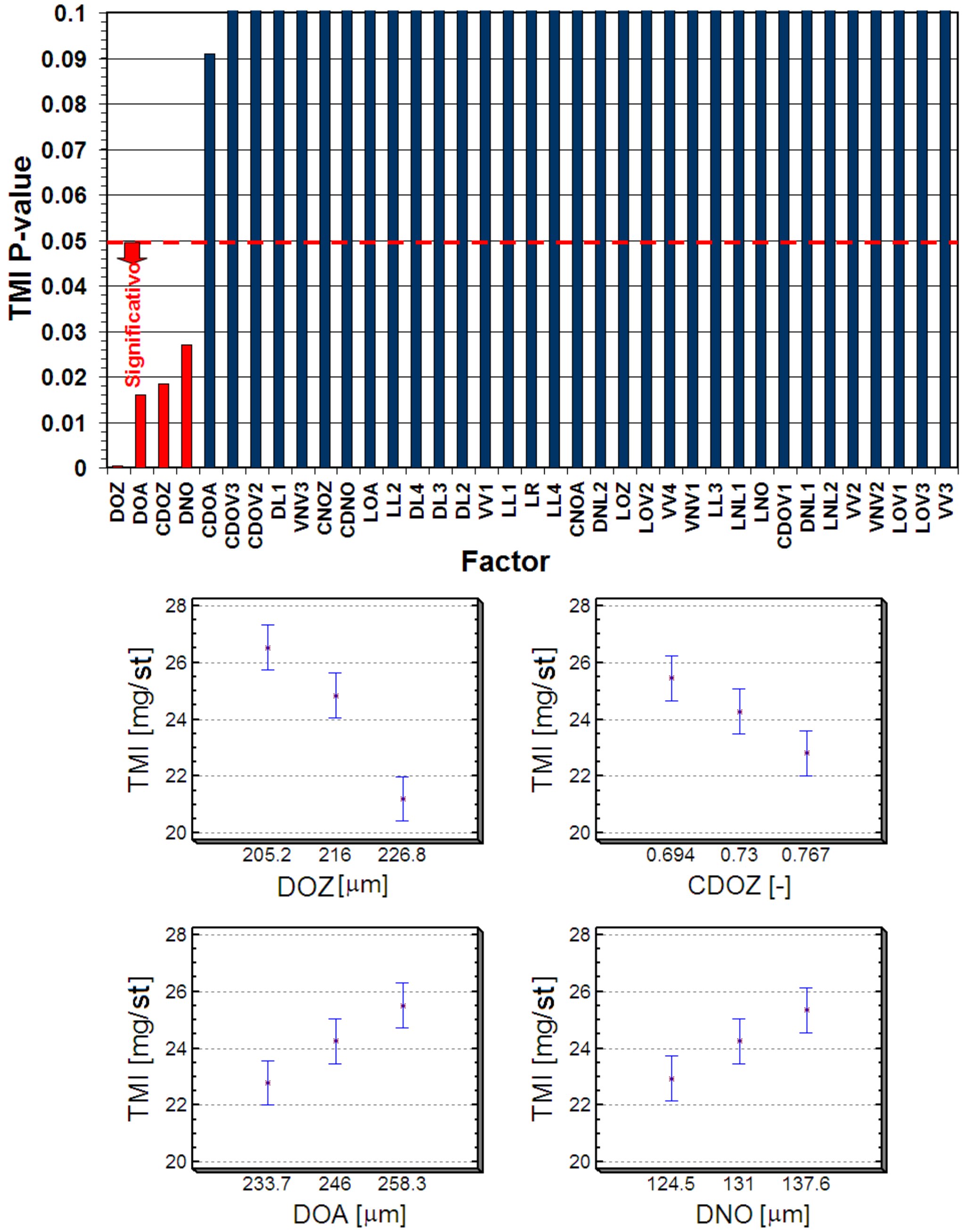

Figure 15. *p-values* for all the geometric parameters and LSD intervals for the significant factors *DOZ*, *CDOZ*, *DOA* and *DNO*.

5.4. Relative importance of non-significant parameters.

As the previous sections pointed out through the analysis of the response variables, the most influencing factors on the injection profile are the control orifices. Their relative importance over the other ones is so high that they may be misleading, suggesting the erroneous conclusion that the rest of factors (about 30) do not bear any importance. In order to contextualize their importance among the rest of parameters, the same plan of simulations has been repeated, in this case without varying any of the parameters relative to the control orifices. Figure 16 shows the mass flow rate profiles obtained under this new constraint after performing the 81 simulations of the L_{81} array involving all the parameters of Table 4 except for those relative to the control orifices (numbered from 21 to 28 in the table).

As it may be appreciated in Figure 16, the variability in mass flow rate profiles is notably reduced when compared to the one shown in Figure 11, especially regarding the opening and closing stages of the signals. Nevertheless, the geometrical factors that were appointed to as non-significant in the previous analysis importantly affect the injection rate. This is due to the fact that the effect of the control orifices in the previous analysis was very large compared to the rest of factors, thus being statistically more significant.

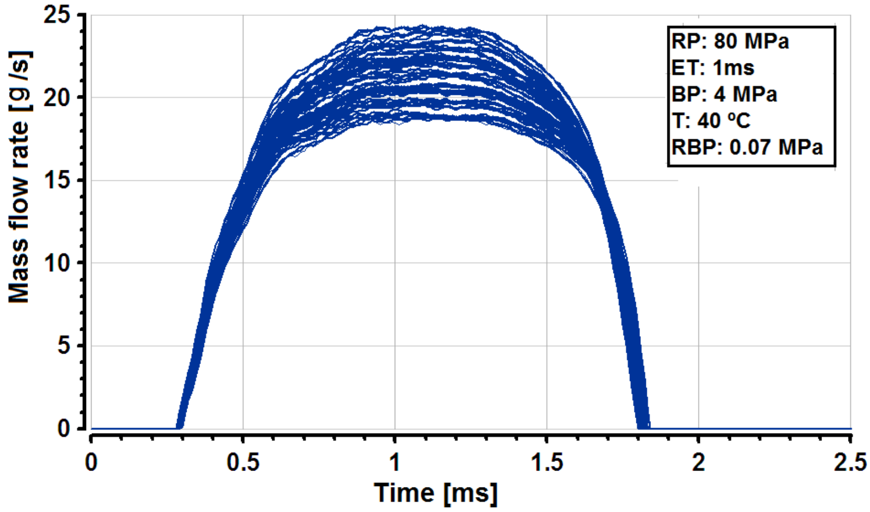

Figure 16. Mass flow rate profiles for the simulations of the L_{81} array without varying any of the parameters related to the control volume orifices.

Figure 17 shows the significant parameters found after these new analysis of variance. As it may be observed, the most significant parameters in this case may be divided in three big groups:

1. Parameters belonging to the solenoid valve.
2. Parameters belonging to the nozzle.
3. Parameters belonging to the injector holder.

The parameters comprised in each of the groups are studied next.

1. Parameters belonging to the solenoid valve.

- Ball valve discharge coefficient (*CDOV2*). This parameter strongly influences the behaviour of the *SOI*, *IT* and *TMI* response variables. The reason has to do with the fact that it produces the same effect as the outlet control orifice. Specifically, it affects the pressure drop in the control volume although to a lower extent. The LSD intervals of this factor on the three response variables represented in Figure 18 clearly show that the delay among the electric signal and the injection (i.e. the *SOI*) is reduced the higher the discharge coefficient of this valve. Additionally, high values of C_d lead to an increase in injection time (*IT*) and total mass injected (*TMI*). A high C_d favours the pressure drop in the control volume, easing the needle rise and consequently the injection rate, as seen in previous sections.

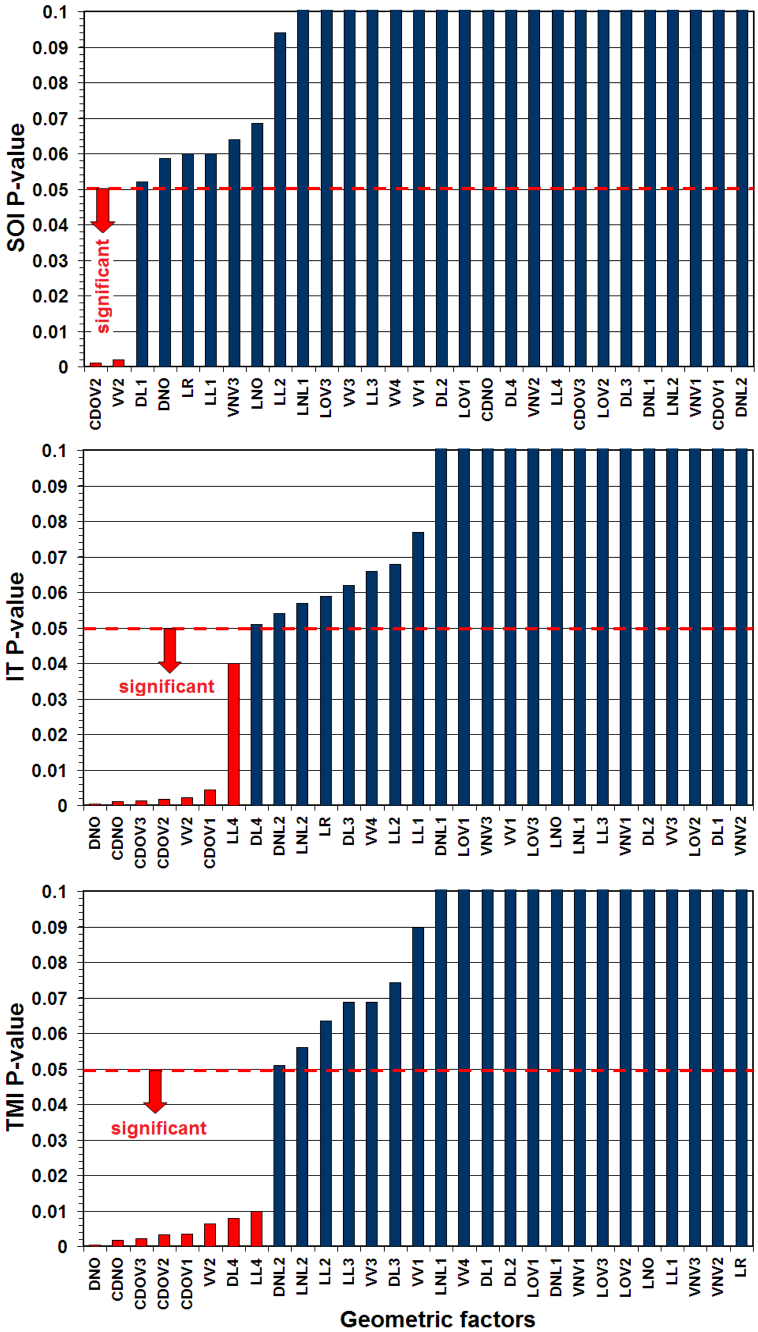

Figure 17. *p-values* for all the geometric factors excluding the parameters of the control orifices.

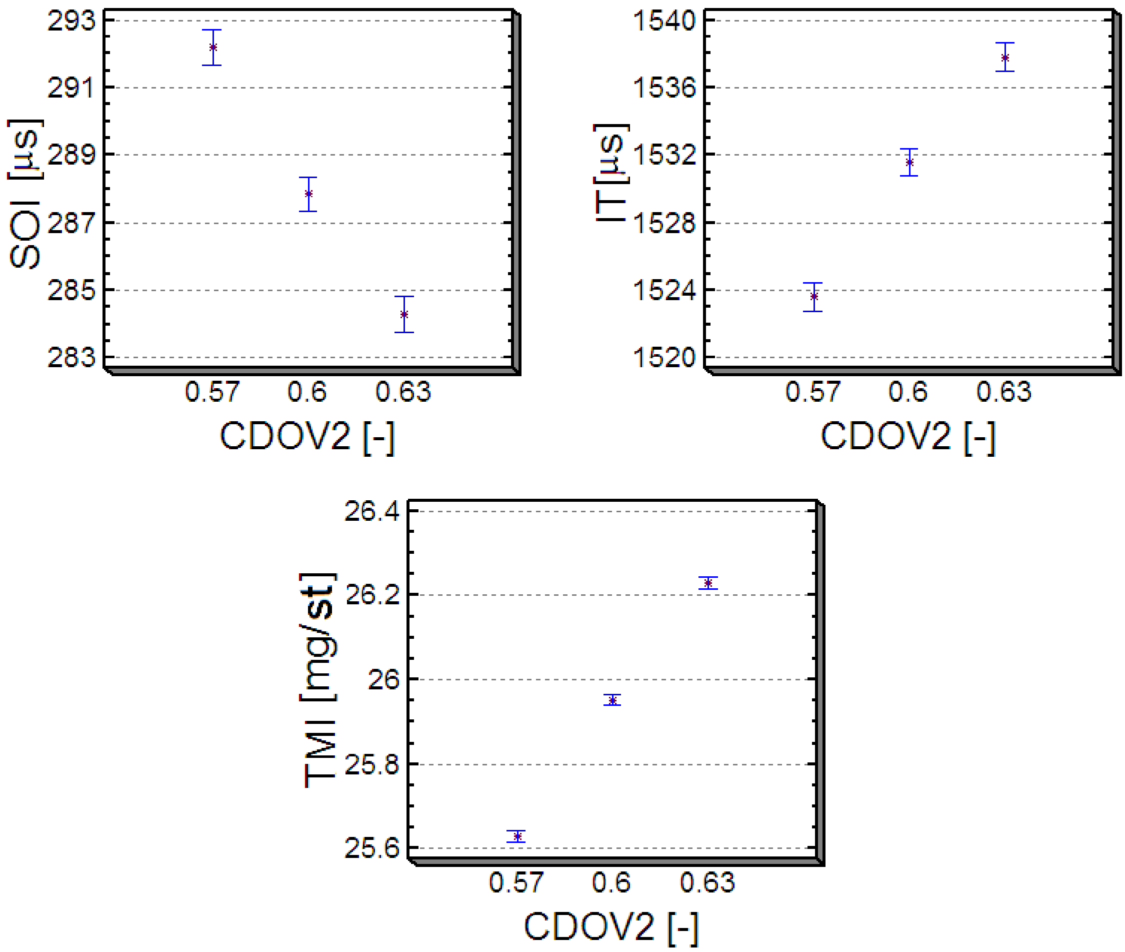

Figure 18. LSD intervals for the *CDOV2* factor.

- Control volume (*VV2*): Given that it is the volume where the pressure drop controlling the rod-needle ensemble is produced, it could be expected that its size had a considerable effect on injector dynamics, as demonstrated by the ANOVA results. Variations of its value substantially change the injection rate profile. If the volume is enlarged, the pressure decrease in it during the injection start (with the *OV2* valve open) is less important, slowing the injector opening. This is the reason why the trend in the design of solenoid operated injectors is to reduce its size (7)(8)(35). Figure 19 shows the LSD intervals related to the variations of this parameter, confirming the explained tendency.

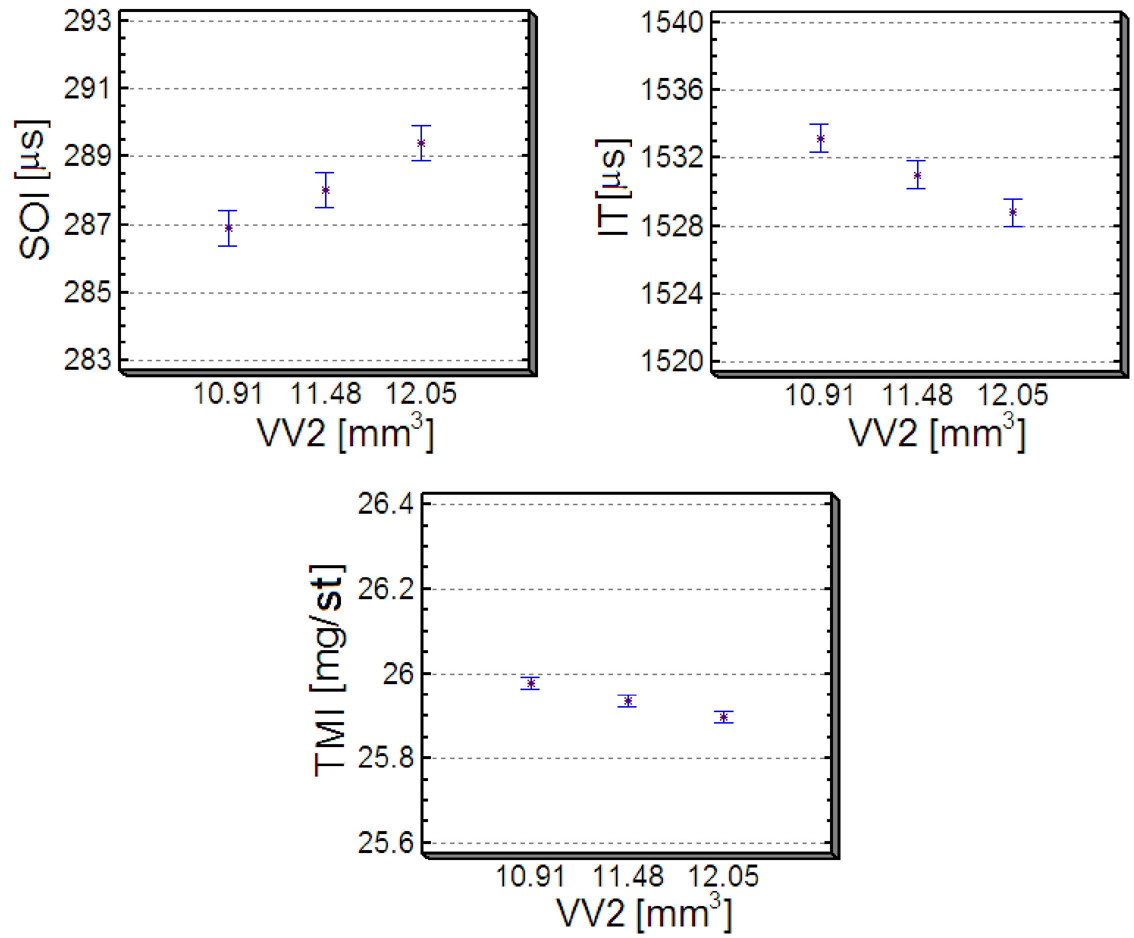

Figure 19. LSD intervals for the *VV2* factor.

- Discharge coefficient of the *OV1* variable orifice (*CDOV1*): this orifice corresponds to the area existing among the body of the ball valve and the upper part of the rod (Figure 2), its variable cross-sectional area depending on the displacement of this last element. This orifice is the link among the inlet and outlet control volume orifices through the volumes *V2* and *V3* (see Figure 2). Even though the variable area of this orifice is way greater than the area of the control volume outlet orifice (*OA*), it influences the upstream pressure thus substantially modifying injector dynamics. Due to this fact, the last generation designs for solenoid injectors have modified this part of the injector (7)(8)(35). The LSD intervals for this parameter are shown in Figure 20. The figure shows that the injection time grows as the discharge coefficient of the variable section orifice *OV1* increases, thus also augmenting the injected mass. On the other hand, it can be seen that this parameter hardly influences the start of injection (*SOI*). The explanation resides in the fact that the area of this variable orifice reaches its maximum value when the needle is resting on its seat. In this situation, its variation is not significant, therefore preventing its influence on the early stages of the injection.

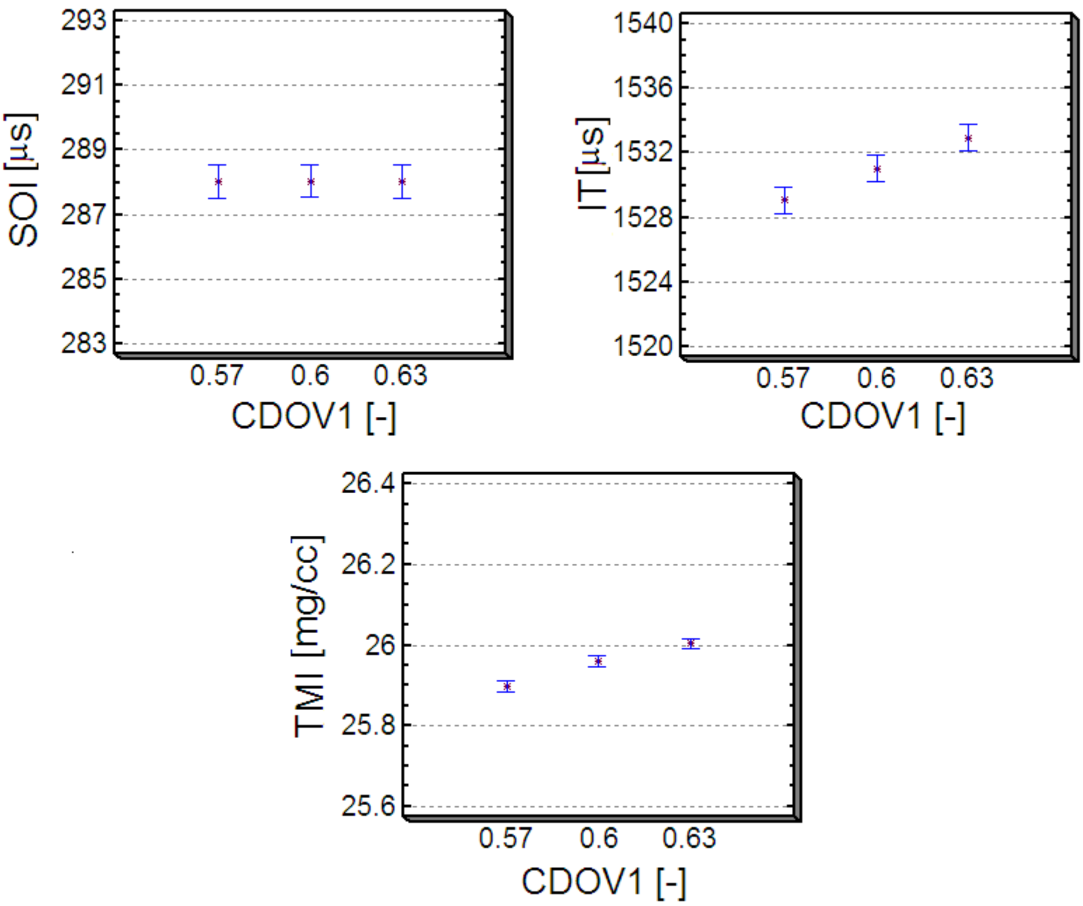

Figure 20. LSD intervals for the *CDOV1* factor.

2. Nozzle parameters.

As Figure 17 reflects, the diameter of the nozzle orifices (*DNO*) and their associated discharge coefficient (*CDNO*) are the parameters with a major influence on the injection time (*IT*) and the total mass injected (*TMI*). Indeed, these factors show the lowest *p-values* for both response variables. However, as the results show, they are not significant as far as the injection delay (*SOI*) is concerned.

As per the influence of these two variables, *DNO* and *CDNO*, they are related to the instantaneous injected mass through Equation (4):

$$\dot{m} = C_d \cdot A_o \cdot \rho_f \cdot \sqrt{\frac{2 \cdot (RP - BP)}{\rho_f}} \qquad (4)$$

This equation governs the behaviour of the injection rate during its steady-state stage. Hence, its influence on the total mass injected is direct. Besides, the discharge coefficient influences the pressure in the *NV3* volume (Figure 1) to a certain extent. This pressure is exerted on the lower side of the needle, thus strongly influencing its dynamics and consequently the injection duration.

3. Injector holder parameters.

As underlined in the view of the ANOVA results (Figure 17), the most significant parameters belonging to the injector holder are the length and diameter of the *L4* internal duct (*DL4* and *LL4*, respectively) (Figure 2). These parameters directly influence the pressure losses along the injector body. Figure 21 provides the LSD intervals of these factors concerning the injection time (*IT*) and total mass injected (*TMI*) response variables. The lower the line diameter and/or the higher its length, the greater the pressure loss along the duct, thus reducing the effective force on the lower side of the needle. As a consequence, the needle lift is reduced and so is the injection time. Nevertheless, as it may be seen in the upper part of Figure 17, it is not a significant factor from the point of view of the start of injection. The reason is that right before the beginning of the injection the fluid is at rest within the injector. On the other hand, as Figure 21 shows, it is important to note that it is much more significant to modify the length in a 5% than the diameter in the same proportion, which is demonstrated due to the higher separation among the LSD intervals for the former factor.

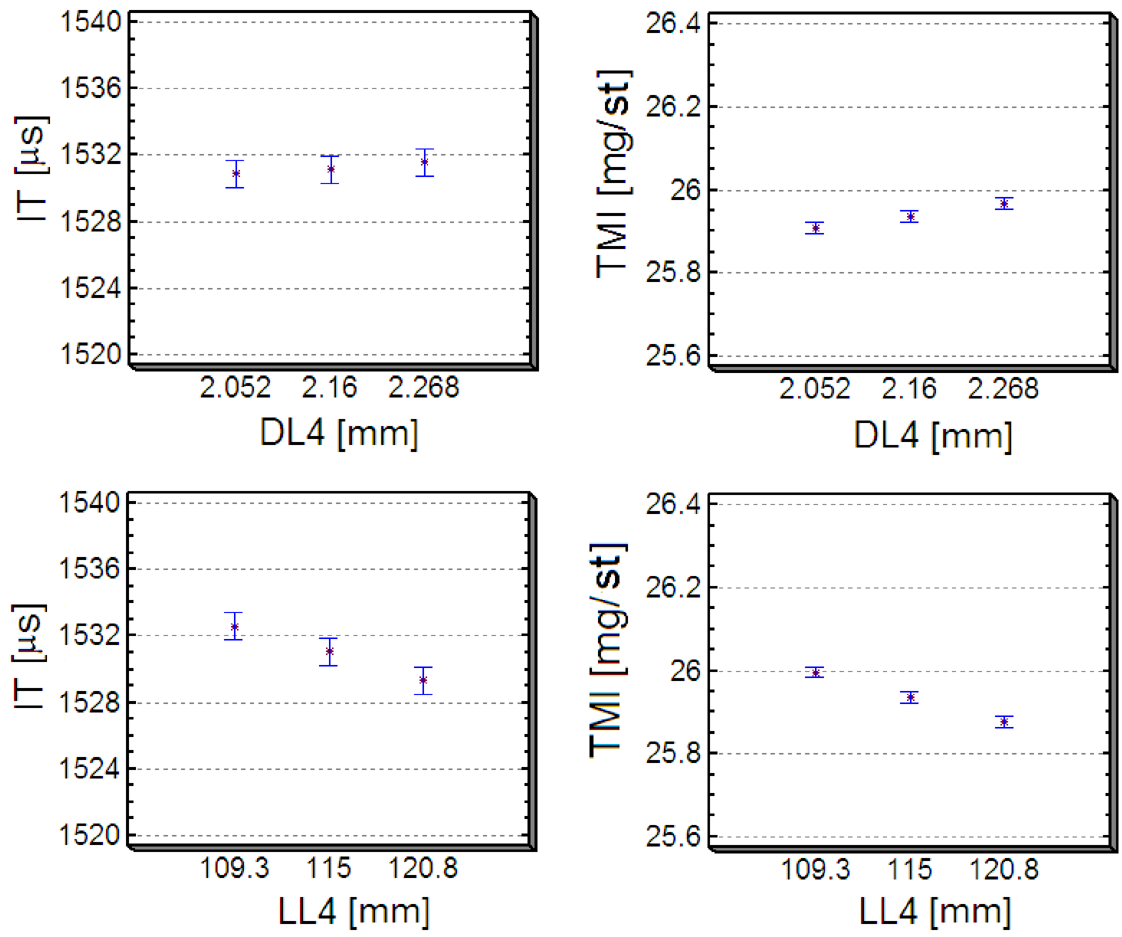

Figure 21. LSD intervals for the *DL4* and *LL4* factors.

6. Conclusions

In the present investigation, a quantification of the influence of deviations from the nominal values of the parameters on the injection rate of diesel injectors has been carried out by conducting an analysis of variance (ANOVA) for a reference operating condition, by means of a previously validated one-dimensional model of a Bosch injector.

On the one hand, some functional parameters (namely the energizing time, rail pressure, discharge pressure, fuel temperature and injector return line pressure) have been taken as factors to be studied. On the other hand, up to 37 different geometrical and flow factors have been considered (23 and 14, respectively).

From the study, it has become clear that the injector performance mainly depends on 6 factors: the rail pressure, the energizing time, the fuel temperature and the permeability of both control orifices and the nozzle (the permeability being defined as the product of the discharge coefficient times the geometrical area of the orifice). As far as the functional parameters are concerned, the rail pressure, energizing time and fuel temperature may be submitted to fluctuations during the normal operation of the injector, making their values depart from the nominal ones. Regarding the geometric and flow parameters, the permeability of the orifices depends on factors such as the accuracy of the manufacturer during the mechanizing process or the injector aging, whose influence should be accounted for. The configuration of the control volume inlet and outlet orifices, together with the discharge coefficient of the inlet orifice, play a key role in the behaviour of the common-rail injectors with a similar design to the one here dealt with. The reason resides in the fact that they are in charge of controlling the pressure in the control volume, which bears great importance in needle dynamics and consequently on the injection process. Variations in the order of 5% in the diameter of these orifices produce a strong change in the fuel injection rate, reflected in terms of total mass injected, delay to the start of injection and duration of the injection process. Results obtained by other authors in the literature are aligned with the ones here presented (13)(36)(37)(38).

Given that the influence of the parameters linked to the control orifice on the injection rate is way greater than the one of any other parameter considered, the third part of the study has been devoted to an additional analysis of variance. In this analysis, the former parameters have been left constant, exclusively considering variations of the other factors. This has allowed to sort and quantify the importance of the rest of parameters. In this part of the study, the configuration of the ball valve parameters has been proved to be of great importance. This has been, in fact, the part of the injector that has suffered most variations in design in the successive generations of injectors during the past years. The study also pointed out that, although to a lower extent, the losses along the injector internal ducts also influence the injector behaviour.

7. Acknowledgements

This research has been partially funded by FEDER and the Spanish “Ministerio de Economía y Competitividad” through the project TRA2015-67679-c2-1-R.

References

1. Payri R, Salvador FJ, Gimeno J, De la Morena J. Influence of injector technology on injection and combustion development, Part 2: Combustion analysis. Appl Energy [Internet]. 2011;88(4):1130–9. Available from: http://www.sciencedirect.com/science/article/pii/S0306261910004071
2. Heywood JB. Internal Combustion Engine Fundamentals. Vol. 21, McGrawHill series in mechanical engineering. 1988. 930 p.
3. Kent JC, Brown GM. Nozzle exit flow, characteristics for square-edged and rounded inlet geometries. Combust Sci Technol. 1983;30:121–32.
4. Desantes JM, Salvador FJ, Lopez JJ, De la Morena J. Study of mass and momentum transfer in diesel sprays based on X-ray mass distribution measurements and on a theoretical derivation. Exp Fluids [Internet]. 2011;50(2):233–46. Available from: http://link.springer.com/article/10.1007/s00348-010-0919-8
5. Lujan JM, Tormos B, Salvador FJ, Gargar K. Comparative analysis of a DI diesel

engine fuelled with biodiesel blends during the European MVEG-A cycle: Preliminary study (I). Biomass and Bioenergy [Internet]. 2009;33(6–7):941–7. Available from: http://linkinghub.elsevier.com/retrieve/pii/S0961953409000403

6. Salvador FJ, Martínez-López J, Caballer M, De Alfonso C. Study of the influence of the needle lift on the internal flow and cavitation phenomenon in diesel injector nozzles by CFD using RANS methods. Energy Convers Manag [Internet]. 2013;66:246–56. Available from: http://dx.doi.org/10.1016/j.enconman.2012.10.011

7. Payri R, Salvador FJ, Martí-Aldaraví P, Martínez-López J. Using one-dimensional modeling to analyze the influence of the use of biodiesels on the dynamic behavior of solenoid-operated injectors in common rail systems: Detailed injection system model. Energy Convers Manag [Internet]. 2012;54(1):90–9. Available from: http://dx.doi.org/10.1016/j.enconman.2011.10.004

8. Payri R, Climent H, Salvador FJ, Favennec A-G. Diesel Injection System Modelling. Methodology and Application for a First-generation Common Rail System. Proc Inst Mech Eng Part D J Automob Eng. 2004;218(1):81–91.

9. Salvador FJ, Gimeno J, De la Morena J, Carreres M. Using one-dimensional modeling to analyze the influence of the use of biodiesels on the dynamic behavior of solenoid-operated injectors in common rail systems: Results of the

simulations and discussion. Energy Convers Manag [Internet]. 2012;54(1):122–32. Available from: http://dx.doi.org/10.1016/j.enconman.2011.10.004

10. Salvador FJ, Plazas AH, Gimeno J, Carreres M. Complete modelling of a piezo actuator last-generation injector for diesel injection systems. Int J Engine Res [Internet]. 2014 Jan 1;15(1):3–19. Available from: http://jer.sagepub.com/content/early/2012/09/06/1468087412455373.abstract

11. Bianchi GM, Falfari S, Brusiani F, Pelloni P. Advanced Modelling of a New Diesel Fast Solenoid Injector and Comparison with Experiments. SAE Tech Pap 2004-01-0019. 2004;

12. Payri R, Tormos B, Salvador FJ, Plazas AH. Using one-dimensional modelling codes to analyse the influence of diesel nozzle geometry on injection rate characteristics. Int J Veh Des. 2005;38(1):58–78.

13. Bianchi GM, Falfari S, Parotto M, Osbat G. Advanced modeling of common rail injector dynamics and comparison with experiments. SAE Pap 2003-01-0006. 2003;

14. Zeh D, Hammer PJ, Uhr C, Rückle M, Rettich A, Grota B, et al. Bosch Diesel Injection Technology – Response for Every Vehicle Class. In: 23rd Aachen Colloquium Automobile and Engine Technology 2014. Aachen; 2014.

15. Ross PJ. Taguchi techniques for quality engineering. Mc, Graw Hill. 1998;

16. Salvador FJ, Gimeno J, Carreres M, Crialesi-Esposito M. Fuel temperature

influence on the performance of a last generation common-rail diesel ballistic injector. Part I: Experimental mass flow rate measurements and discussion. Energy Convers Manag [Internet]. 2016 Apr;114:364–75. Available from: http://dx.doi.org/10.1016/j.enconman.2016.02.042

17. Payri R, Salvador FJ, Carreres M, De la Morena J. Fuel temperature influence on the performance of a last generation common-rail diesel ballistic injector. Part II: 1D model development, validation and analysis. Energy Convers Manag [Internet]. 2016 Apr;114:376–91. Available from: http://dx.doi.org/10.1016/j.enconman.2016.02.043

18. Nurick WH. Orifice cavitation and its effects on spray mixing. J Fluids Eng. 1976;98:681–7.

19. Soteriou C, Andrews R, Smith M. Further studies of cavitation and atomization in Diesel injection. SAE Pap 1999-01-1486. 1999;

20. Payri F, Payri R, Salvador FJ, Martínez-López J. A contribution to the understanding of cavitation effects in Diesel injector nozzles through a combined experimental and computational investigation. Comput Fluids [Internet]. 2012 Apr;58:88–101. Available from: http://dx.doi.org/10.1016/j.compfluid.2012.01.005

21. Salvador FJ, Hoyas S, Novella R, Martínez-López J. Numerical simulation and extended validation of two-phase compressible flow in diesel injector nozzles.

Proc Inst Mech Eng Part D J Automob Eng. 2011;225(4):545–63.

22. Salvador FJ, Romero J V., Roselló MD, Martínez-López J. Validation of a code for modeling cavitation phenomena in Diesel injector nozzles. Math Comput Model [Internet]. 2010;52(7–8):1123–32. Available from: http://www.sciencedirect.com/science/article/pii/S0895717710000919

23. Lopez JJ, Salvador FJ, De la Garza OA, Arrègle J. A comprehensive study on the effect of cavitation on injection velocity in diesel nozzles. Energy Convers Manag. 2012;64:415–23.

24. Salvador FJ, Martínez-López J, Romero J V., Roselló MD. Computational study of the cavitation phenomenon and its interaction with the turbulence developed in diesel injector nozzles by Large Eddy Simulation (LES). Math Comput Model [Internet]. 2013;57(7–8):1656–62. Available from: http://dx.doi.org/10.1016/j.mcm.2011.10.050

25. Chaves H, Knapp M, Kubitzek A, Obermeier F. Experimental study of cavitation in the nozzle hole of diesel injectors using transparent nozzles. SAE Pap 950290. 1995;

26. Giannadakis E, Gavaises M, Roth H. Cavitation Modelling in Single-Hole Diesel Injector Based on Eulerian-Lagrangian Approach. In: THIESEL 2004 Conference on Thermo- and Fluid Dynamic Processes in Diesel Engines [Internet]. 2004. p. 1–13. Available from:

http://scholar.google.com/scholar?hl=en&btnG=Search&q=intitle:Cavitation+Modelling+in+Single-Hole+Diesel+Injector+Based+on+Eulerian-Lagrangian+Approach#0

27. Ohrn TR, Senser DW, Lefèbvre AH. Geometrical effects on discharge coefficients for plain-orifice atomizers. At Sprays. 1991;1(2):137–53.

28. Lichtarowicz AK, Duggins RK, Markland E. Discharge coefficients for incompressible non-cavitating flow through long orifices. J Mech Engng Sci. 1965;7(2):210–9.

29. Fox TA, Stark J. Discharge coefficients for miniature fuel injectors. Proc Inst Mech Engrs. 1989;203:75–8.

30. Molina S, Salvador FJ, Carreres M, Jaramillo D. A computational investigation on the influence of the use of elliptical orifices on the inner nozzle flow and cavitation development in diesel injector nozzles. Energy Convers Manag [Internet]. 2014;79:114–27. Available from: http://linkinghub.elsevier.com/retrieve/pii/S0196890413007917

31. Salvador FJ, Carreres M, Jaramillo D, Martínez-López J. Analysis of the combined effect of hydrogrinding process and inclination angle on hydraulic performance of diesel injection nozzles. Energy Convers Manag [Internet]. 2015;105:1352–65. Available from: http://dx.doi.org/10.1016/j.enconman.2015.08.035

32. Tafreshi H V, Pourdeyhimi B. Simulating cavitation and hydraulic flip inside hydroentangling nozzles. Text Res J [Internet]. 2004;74:359–64. Available from: http://www.vcu.edu/

33. Habchi C, Dumont N, Simonin O, Soteriou C, Torres N, Andrews R. Multidimensional simulation of cavitating flows in diesel injectors by a homogeneous mixture modeling approach. At Sprays [Internet]. 2008;18:129–62. Available from: http://www.dl.begellhouse.com/journals/6a7c7e10642258cc,3bcb27ce5a5a256c,18a21cfb6373644a.html

34. Salvador FJ, Carreres M, Jaramillo D, Martínez-López J. Comparison of microsac and VCO diesel injector nozzles in terms of internal nozzle flow characteristics. Energy Convers Manag [Internet]. 2015;103:284–99. Available from: http://linkinghub.elsevier.com/retrieve/pii/S0196890415005270

35. Zeh D, Hammer J, Uhr C, Rückle M, Rettich A, Grota B, et al. Bosch Diesel Injection Technology – Response for Every Vehicle Class Production. In: 23rd Aachen Colloquium Automobile and Engine Technology 2014. Aachen; 2014.

36. Bianchi G, Falfari S, Brusiani F, Pelloni P, Osbat G, Parotto M. Numerical Investigation of Critical Issues in Multiple-Injection Strategy Operated by a New CR Fast-Actuation Solenoid Injector. SAE Tech Pap 2005-01-1236 [Internet]. 2005; Available from:

http://scholar.google.com/scholar?hl=en&btnG=Search&q=intitle:Numerical+Investigation+of+Critical+Issues+in+Multiple-Injection+Strategy+Operated+by+a+New+C+.+R+.+Fast-Actuation+Solenoid+Injector#0

37. Ficarella A, Laforgia D. Injection characteristics simulation and analysis in diesel engines. Meccanica [Internet]. 1993 Sep;28(3):239–48. Available from: http://link.springer.com/article/10.1007%2FBF00989127

38. Desantes JM, Arrègle J, Rodríguez P. Computational model for simulation of Diesel Injection systems. SAE Pap 1999-01-0915. 1999;